

**PROGRESS TOWARDS CO-CRYSTALLIZATION OF THE *E. COLI*
MEMBRANE PROTEIN INTIMIN WITH ENGINEERED PEPTIDE-
SPECIFIC ANTIBODY FRAGMENTS**

A Thesis
Presented to
The Academic Faculty

by

David Prince Heaner Jr.

In Partial Fulfillment
of the Requirements for the Degree
B.S. Chemistry with the Research Option
In the School of Chemistry & Biochemistry

Georgia Institute of Technology
December 2015

COPYRIGHT 2015 BY DAVID PRINCE HEANER JR.

**PROGRESS TOWARDS CO-CRYSTALLIZATION OF THE *E. COLI*
MEMBRANE PROTEIN INTIMIN WITH ENGINEERED PEPTIDE-
SPECIFIC ANTIBODY FRAGMENTS**

Approved by:

Dr. Raquel Lieberman, Advisor
School of Chemistry & Biochemistry
Georgia Institute of Technology

Dr. Ingeborg Schmidt-Krey
School of Chemistry & Biochemistry
Georgia Institute of Technology

Date Approved: April 17, 2015

This thesis work is dedicated to:

David P. Heaner Sr.

Anita Heaner

Canada Heaner

Ron Monroe

Willetta Monroe

John D. Huckabee

Maxine Heaner Huckabee

William L. Heaner Jr.

Thank you for your love and support

ACKNOWLEDGEMENTS

I would like to thank first and foremost my principal investigator Dr. Raquel Lieberman for allowing me to become a member of her laboratory as a first year. She provided me with invaluable laboratory experience, professional mentorship and support throughout my time in her lab. I would like to thank my graduate student advisor Sibel Kalyoncu (PhD candidate) for her assistance with experimental design, data collection, and professional guidance. Sibel took on her role as my mentor while just a second semester international graduate student. She has unquestionably facilitated my growth over the past 4 years. I wish to thank Jennifer Johnson (PhD candidate) and Ivan Morales (undergraduate alumnus) for their support and contributions to the project discussed in this work. I would also like to acknowledge the Petit Scholars Program for their support throughout the course of the project. To all the members of Lieberman lab, past and present, I sincerely thank you for your support and friendship that will always be a part of my Georgia Tech undergraduate experience.

TABLE OF CONTENTS

	Page
ACKNOWLEDGEMENTS	iv
LIST OF TABLES	viii
LIST OF FIGURES	ix
LIST OF SYMBOLS AND ABBREVIATIONS	x
SUMMARY	xii
<u>CHAPTER</u>	
1 INTRODUCTION	1
2 PURIFICATION AND CHARACTERIZATION OF SCFV/EE VARIANTS AND FAB/EE ANTIBODY FRAGMENTS	7
Abstract	7
Introduction	7
Experimental	9
ScFv/EE & Fab/EE Plasmids	9
Expression of scFv/EE Variants	9
Purification of scFv/EE Variants	10
Expression of Fab/EE	11
Purification of Fab/EE	11
Results & Discussion	12
ScFv/EE and Fab/EE Antibody Fragments	12
3 PROTEIN ENGINEERING, EXPRESSION, AND PURIFICATION OF THE INTIMIN VARIANTS	17
Abstract	17

Introduction	17
Experimental	18
Intimin Plasmid	18
Intimin-EE Protein Engineering	19
Expression of the Intimin Variants	19
Purification of the Intimin Variants	20
Results & Discussion	21
Intimin-EE Protein Engineering	21
Expression and Purification of the Intimin Variants	23
4 COMPLEXATION OF THE INTIMIN-EE VARIANTS WITH THE	26
SCFV/EE AND FAB/EE ANTIBODY FRAGMENTS	
Abstract	26
Introduction	26
Experimental	27
Intimin-EE & ScFv/EE Complex Formation	27
Intimin-EE & Fab/EE Complex Formation	27
Results & Discussion	28
Complexation of Intimin-EE & ScFv/EE Variants	28
Complexation of Intimin-EE & Fab/EE	35
5 CO-CRYSTALLIZATION OF INTIMIN-EE WITH THE	37
SCFV/EE AND FAB/EE ANTIBODY FRAGMENTS	
Abstract	37
Introduction	38
Experimental	38
Results & Discussion	39

Co-crystallization Trials of Intimin-EE7 & ScFv/EE.k	39
Co-crystallization Trials of Intimin-EE8 & Fab/EE	40
Co-crystallization Trials of Intimin-EE7 & Fab/EE	44
6 CONCLUSIONS AND FUTURE DIRECTIONS FOR EYMPME	47
PEPTIDE-SPECIFIC CO-CRYSTALLIZATION OF INTIMIN	
APPENDIX A: CHAPTER 2 SUPPLEMENTARY	52
APPENDIX B: CHAPTER 3 SUPPLEMENTARY	54
Protein Engineering of Intimin-EE Variants	54
Expressions and Purification of Intimin-EE Variants	55
APPENDIX C: CHAPTER 4 SUPPLEMENTARY	58
APPENDIX D: CHAPTER 5 SUPPLEMENTARY	59
REFERENCES	67
VITA	70

LIST OF TABLES

	Page
Table A.1: ScFv/EE.k and Fab/EE Protein Yields	53
Table B.1: Intimin-EE Oligonucleotide Primer Sequences	55
Table B.2: LDAO Solubilized Intimin Variant Protein Yields	57
Table B.3: DDM Solubilized Intimin Variant Protein Yields	57
Table C.1: All Intimin-EE and ScFv/EE Variant S300 Complexations	58
Table C.2: All Intimin-EE and ScFv/EE.k S12 Complexations	58
Table D.1: Co-crystallization Trays Prepared for DDM Solubilized Intimin-EE7 & ScFv/EE.k	59
Table D.2: Co-crystallization Trays Prepared for DDM Solubilized Intimin-EE7 & ScFv/EE.k Continuation	60
Table D.3: Co-crystallization Trays Prepared for DDM Solubilized Intimin-EE8 & Fab/EE	61
Table D.4: Co-crystallization Trays Prepared for DDM Solubilized Intimin-EE8 & Fab/EE Continuation	62
Table D.5: Co-crystallization Trays of the DMPC/CHAPSO bicelle Solubilized Intimin-EE8 & Fab/EE	63
Table D.6: LCP Trays Prepared for Intimin-EE8 & Fab/EE	63
Table D.7: Co-crystallization Trays Prepared for DDM Solubilized Intimin-EE7 & Fab/EE	64
Table D.8: Co-crystallization Trays Prepared for DDM Solubilized Intimin-EE7 & Fab/EE Continuation	65
Table D.9: Co-crystallization Trays Prepared for DDM Solubilized Intimin-EE7 & Fab/EE Continuation	66
Table D.10: LCP Trays Prepared for Intimin-EE7 & Fab/EE	66

LIST OF FIGURES

	Page
Figure 1.1: IgG Antibody Fragments	3
Figure 1.2: Proposed Peptide-Specific Co-crystallization	5
Figure 1.3: Model Membrane Protein Intimin	6
Figure 2.1: ScFv/EE.k and Fab/EE SDS-PAGE	12
Figure 2.2: Engineered Single Chain Antibody Fragment Crystal Lattices	14
Figure 2.3: Engineered Fab Fragment Crystal Lattice	15
Figure 3.1: Intimin-EE Variants	22
Figure 3.2: Intimin-EE Variants SDS-PAGE Gels	24
Figure 4.1: Intimin-EE and scFv/EE.k S300 Complexations	29
Figure 4.2: Intimin-EE and scFv/EE.k S12 Complexations	32
Figure 4.3: Detergent Chemical Structures	34
Figure 4.4: Intimin-EE and Fab/EE S12 Complexations	36
Figure 5.1: Intimin-EE8 and Fab/EE Co-crystal Hit	41
Figure 5.2: Intimin-EE7 and Fab/EE Co-crystal Hit	45
Figure 6.1: Molecular Dynamics of Intimin-EE and Fab/EE	51
Figure A.1: ScFv/EE.k and Fab/EE Purification Chromatograms	52
Figure A.2: Oligomeric Analysis of ScFv Variants	53
Figure B.1: Primary Protein Structure of Intimin Variants	54
Figure B.2: Intimin-EE Variant Expression	55
Figure B.3: Intimin Variant Purification Chromatograms	56
Figure D.1: Diffraction of Intimin-EE7 and Fab/EE Co-crystal Hit	59

LIST OF SYMBOLS AND ABBREVIATIONS

ScFv	Single chain antibody fragment
EE	Hexapeptide sequence EYMPME
scFv/His	Anti-His ₆ ScFv
scFv/EE	First generation anti-EE ScFv
scFv/EE.k	Second generation anti-EE ScFv
scFv/EE.a	Second generation anti-EE ScFv
Fab/EE	Anti-EE Fab antibody fragment
IMP	Integral Membrane Protein
NYCOMPS	The New York Consortium on Membrane Protein Structure
SEC	Surface Entropy Reduction
ELISA	Enzyme-Linked Immunosorbant Assay
SDM	Site Directed Mutagenesis
CDR	Complementarity Determining Regions
LB	Luria Broth
CAM	Chloramphenicol
TB	Terrific Broth
IPTG	isopropyl- β -D-1-thiogalactopyranoside
EDTA	Ethylenediaminetetraacetic acid
GF	Gel filtration
Sup75	Superdex 75 GF column
AMP	Ampicillin
KAN	Kanamycin
SDS-PAGE	Sodium Dodecyl Sulfate Polyacrylamide Gel Electrophoresis

WT	Wild Type
Intimin-EE	EE containing intimin protein
T_m	Melting temperature
S300	Sephacryl 300 GF column
S12	Superose 12 GF column
LDAO	Lauryldimethylamine-N-oxide
DDM	n-dodecyl- β -D-maltopyranoside
FC-12	Fos-Choline-12
CMC	Critical Micelle Concentration
LCP	Lipidic Cubic Phases
DMPC/CHAPSO	1,2-Dimyristoyl- <i>sn</i> -glycero-3-phosphocholine/ 3-([3-cholamidopropyl]dimethylammonio)-2-hydroxy-1-propanesulfonate
NaOAc	Sodium acetate
MPD	2-methyl-2,4-pentanediol
TMAO	Trimethylamine-N-oxide
PEG (#)	Polyethylene glycol (Average molecular weight)
PEG MME (#)	Polyethylene glycol monomethyl ether (Average molecular weight)
DMSO	Dimethyl sulfoxide
PDB	Protein Data Bank
HBS	HEPES Buffered Saline
Southeast Regional Collaborative Access Team	SER-CAT

SUMMARY

The determination of membrane protein structures is critical for the development of new pharmaceutical agents. Conventionally, membrane proteins are solubilized by the use of mild detergents. However, due to the lack of hydrophilic residues available to make crystal contacts and interference by the large detergent micelle, the quality of diffraction and resolution level needed for de novo structure determination is usually not obtained. In addition to the conventional detergent method, a new method using engineered single chain antibody fragments (scFv) and a Fab antibody fragment have been developed for use as crystallization chaperones. The scFv and Fab fragment interact with the membrane protein of interest via the EYMPME (EE) tag, which is selectively mutated into a hydrophilic loop of the protein. The membrane protein-antibody fragment complex may enter crystallization trials with the antibody fragment driving the complex nucleation through the formation of numerous, strong crystal contacts. Such a co-crystallization method with anti-EE scFv and Fab fragments provides the protein crystallographer with a “crystallization toolbox” that can be used for any crystallographic study of a protein of interest. Through size exclusion chromatography and SDS-PAGE analysis, complexation of the β -barrel membrane protein intimin harboring the EE tag with scFv/EE and Fab/EE has been shown to occur, from which crystallization trials have ensued. Formation of a co-crystal has proven to be difficult, which can be explained in part through molecular dynamics simulations of the mutated intimin L4 loop. This thesis work will present results and conclusions for this novel co-crystallization method.

CHAPTER 1

INTRODUCTION

Macromolecular crystallization is the biochemical discipline dedicated to the determination of the three dimensional structures of proteins and nucleic acids. Since the deduction of the first protein atomic model of sperm whale myoglobin by J.C. Kendrew in 1958,⁽¹⁾ over 107,000 protein structures have been solved, all compiled in the Protein Data Bank (PDB). Generally, proteins are classified as being soluble or membrane associated. Integral membrane proteins (IMPs) are macromolecules that span the lipid bilayers of prokaryotic and eukaryotic organisms. Such proteins have a wide array of functions including, but not limited to: ion transport, signal transduction, and intercellular recognition and communication. In sequenced genomes, approximately 30% of genes encode for membrane proteins, and nearly 60% of all current pharmaceutical agents target membrane proteins.⁽²⁾ Despite their essential roles in cells and their importance in understanding disease onset and treatment, less than 1% of all known protein structures are membrane proteins.⁽³⁾

Because of the underrepresentation of membrane protein structures, high-throughput expression, purification, and crystallization methodologies have been introduced in the literature,^(4, 5) and consortiums have been created such as The New York Consortium on Membrane Protein Structure (NYCOMPS).⁽⁶⁾ Such methodologies and associations are necessary because expression, purification, and crystallization of IMPs has proven to be notoriously difficult. Recombinant expression of the membrane protein of interest within a host such as *E. coli* can be a challenge. Cell growth yields and

consequently protein yields are often low due to natural low expression of the gene, and the potentially toxic effects that may be induced due to the high abundance of the recombinant membrane protein.⁽³⁾ Due to the high hydrophobic content of a membrane protein, its purification requires solubilization by an amphiphilic agent, conventionally being mild detergent micelles. In order for the determined structure of the protein to be significant, it must be in its natural, folded form. Therefore, the detergent micelle must be able to stabilize the proteins tertiary structure in a Protein-Detergent Complex (PDC). Finding such a detergent normally requires intensive screening and optimization.⁽³⁾

Crystallization of the protein is difficult due to low protein yields, low abundance of strong, hydrophilic crystal contacts, and the challenges introduced by the detergent. The conventional use of detergent micelles introduces at least four challenges to crystallization. The protein may not be stable in the PDC, the phase and intermolecular interactions of the detergent during crystallization must be known to deduce the crystal lattice structure, the covered hydrophobic sections are flexible hindering the formation of crystal contacts, and crystal optimization is difficult thereby limiting the possible resolution of the crystal.⁽⁶⁾

Because of these challenges at the crystallization level, much research has been dedicated to altering the amphiphilic environment surrounding the membrane protein. Greater mimics of the natural lipid environment of a cell membrane can stabilize the protein, thereby increasing the probability of nucleation. Artificial lipid environments such as lipidic cubic phases (LCP) and detergent bicelles have been developed^(7, 8) and have been influential in the structure determination of G-protein Coupled Receptor proteins (GPCRs), ion channels, and other integral membrane proteins such as murine

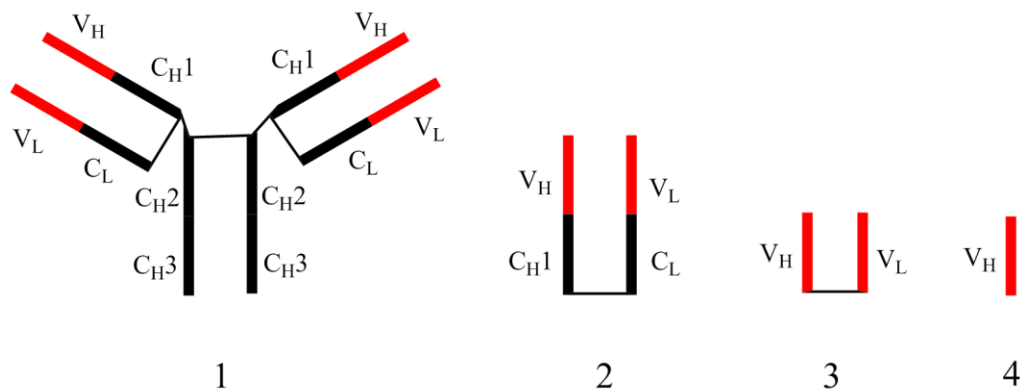


Figure 1.1 IgG Antibody Fragments

Because of their high specificity, monoclonal antibody fragments are common non-covalent chaperones. (1) Intact IgG antibody (2) Fab antibody fragment consisting of heavy and light chain constant regions with intact variable regions. (3) Single chain antibody fragment (scFv) with variable regions connected by a flexible linker. (4) nanobody consisting solely of variable heavy region.

VDAC1.^(9, 10) Finally, protein engineering techniques such as the excision of flexible loop regions,⁽¹¹⁾ and Surface Entropy Reduction (SEC)⁽¹²⁾ have been used to ease membrane protein crystal formation.

As a complement and/or alternative to optimizing the amphiphilic environment and protein engineering is increasing the crystal contacts by covalent and/or non-covalent crystallization chaperones. Although covalent chaperones such as T4 lysozyme have been used in the structure determination of GPCRs, notably the Nobel-Prize winning β_2 Adrenergic G Protein-Coupled Receptor structure,^(9, 13) the method is critically dependent upon the location of the chaperone and it may alter the structure/function of the membrane protein.⁽³⁾ Monoclonal antibody fragments are common non-covalent chaperones (Figure 1.1). Monoclonal Fab and nanobody fragments have been used as crystallization chaperones and protein complex stabilizers such as for the KcsA potassium channel and β_2 adrenergic-Gs protein complex.^(13, 14) Traditionally, the method of identification and production of monoclonal antibodies has been through hybridoma

techniques. In such cases, mice are injected with the protein of interest, and the mouse's immune system creates antibodies against the protein of interest. Splenic B cells are harvested and fused with a myeloma cell line, followed by isolation of the created hybridoma line.⁽¹⁵⁾ Antibodies that bind to the membrane protein are then identified through an enzyme-linked immunosorbant assay (ELISA), and the fragment of interest generated by proteolysis. However, due to the necessity of immunization and creation of hybridomic cell lines, hybridoma techniques are both a time and financial burden.⁽³⁾ Additionally, the raised monoclonal antibody fragment can only recognize one protein target (Figure 1.2). A recent circumvention of animal immunization are molecular display techniques with antibody library panning. In such a system, a pre-existing antibody fragment is selected, and a library is created in which the pre-existing antibody CDR's are diversified and cloned into a phagemid vector.⁽³⁾ After phage infection of *E. coli*, the chaperone is expressed on the viral coat surface, and the phages are allowed to pass over an immobilized, purified membrane protein.⁽³⁾ The cycle is repeated and several high-affinity chaperones are isolated. Molecular display and antibody library selection is a more high-throughput method for the identification of monoclonal antibody fragments against a client protein.⁽³⁾ However, this method is still limited to the one-chaperone-one-protein methodology (Figure 1.2).

As an alternative to the hybridoma and molecular display techniques for non-covalent chaperone identification, more generalized antibody fragments that can recognize multiple protein targets have been envisioned. Principally, engineered, hypercrystallizable Fab and single chain antibody fragments (scFv) have been investigated. These antibody fragments have been engineered to contain

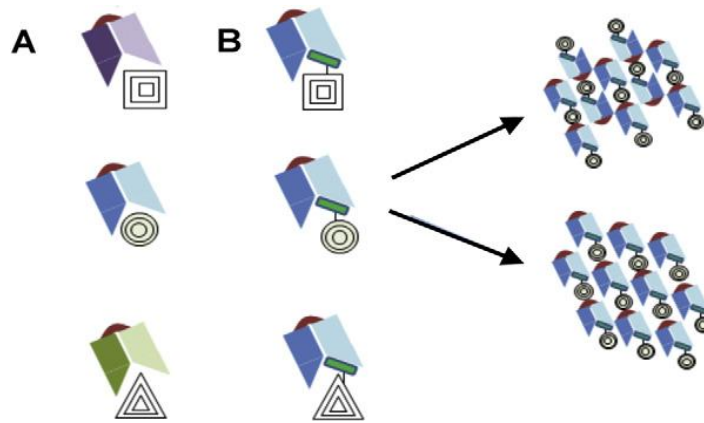


Figure 1.2 Proposed Co-crystallization Approach

- (A) Non-covalent chaperones developed with hybridoma immunization techniques or molecular display with library panning techniques recognize a single protein target.
- (B) Peptide-specific monoclonal antibody fragments can recognize multiple protein targets containing the peptide-specific sequence. Antibody fragments specific to the hexapeptide EYMPME have been developed for co-crystallization with membrane proteins. Figure from Lieberman et al.⁽³⁾

complementarity determining regions (CDR) that recognize a specific hexapeptide epitope EYMPME (EE) that can be mutated into an extramembranous loop of an IMP by site directed mutagenesis (SDM). Through the EE interaction, a protein complex will be formed containing both the antibody fragment and membrane protein. Even though the membrane protein is still solubilized in a detergent micelle, the hypercrystallizable anti-EE Fab (Fab/EE) or anti-EE scFv (scFv/EE) will drive the nucleation of the complex by forming strong crystal contacts with neighboring antibody fragments. Such Fab/EE and scFv/EE proteins have been engineered and their structures determined by Pai et al.⁽¹⁶⁾, Kalyoncu et al.⁽¹⁷⁾, and Johnson et al.⁽¹⁸⁾ In theory, this method can be used for any membrane protein of interest, eliminating the need for new antibody fragments for each new target protein (Figure 1.2).

As a proof of concept for this EE co-crystallization method, variants of the β -barrel membrane protein intimin containing the EE tag have been developed. Intimin is a virulent membrane protein found in the outer membrane of gram-negative bacteria such as *E. coli*.⁽¹⁹⁾

The structure of wild type (WT) intimin was solved by Fairman et al.⁽¹⁹⁾ Complexation trials of the intimin-EE variants with scFv/EE and Fab/EE has shown complex formation to occur. Crystallization trials have ensued for both the Intimin-EE & Fab/EE complex, and Intimin-EE & scFv/EE variant complex.

The objective of this work is fivefold, with each objective covered in a separate chapter. Chapter 2 presents purification and characterization of the scFv/EE and Fab/EE fragments. Chapter 3 covers the development and purification of the intimin-EE variants. Chapter 4 includes the complexation data for both the Intimin-EE & Fab/EE and Intimin-EE & scFv/EE variant complexes. Chapter 5 details the co-crystallization trials for the intimin-EE & Fab/EE and intimin-EE & scFv/EE variant complexes. Chapter 6 concludes the work with a discussion on the feasibility of this co-crystallization approach for intimin-EE along with its future directions.

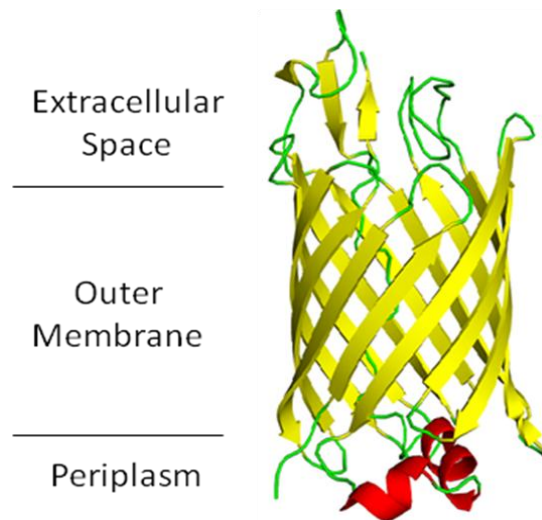


Figure 1.3. Model Membrane Protein Intimin
For co-crystallization trials with the anti-EE antibody fragments, the *E. coli* membrane protein has been selected as the model membrane protein. The WT intimin structure was solved by Fairman et al.

CHAPTER 2

PURIFICATION AND CHARACTERIZATION OF SCFV/EE VARIANTS AND FAB/EE ANTIBODY FRAGMENTS

Abstract

Monoclonal antibody fragments are increasingly being explored for acting as co-crystallization chaperones for IMPs. Such antibody fragments include single chain antibody fragments (scFv), Fab fragments, and nanobodies. Novel characteristics for such chaperones would be hypercrystallizability, enhanced biophysical characteristics, and high protein yields. In this chapter, engineered, hypercrystallizable scFv and Fab fragments are described that have complementarity determining regions specific to the hexapeptide sequence EYMPME (EE). In total, three scFv/EE variants and one Fab/EE variant were developed as outlined by Pai et al.,⁽¹⁶⁾ Kalyoncu et al.,⁽¹⁷⁾ and Johnson et al.⁽¹⁸⁾ These anti-EE antibody fragments were used for complexation and crystallization trials with the EE-tagged *E. coli* outer membrane protein intimin.

Introduction

As a means to increase the hydrophilic surface area of a membrane protein, and thus increasing the number of crystal contacts, non-covalent soluble proteins can form a complex with the membrane protein. Because specificity is critical to forming a complex with the membrane protein of interest, monoclonal antibody fragments are increasingly being used as non-covalent co-crystallization chaperones. Such antibody fragments include single chain antibody fragments (scFv), nanobodies, and Fab fragments (Figure 1.1); with the latter being the most successful chaperone as document in the literature. To

date, the most used techniques for generating these fragments is either by hybridoma techniques or molecular display techniques.

Traditionally, for every new target membrane protein a new chaperone is required (one-protein-one-chaperone). In order to generalize this approach, non-conserved, extramembranous loop regions of the membrane protein are mutated to contain a specific peptide sequence that is recognized by the CDRs of an engineered antibody fragment. Such a model allows for the same antibody fragment to be used for multiple protein targets. In contrast to the initial attempts for peptide-specific co-crystallization through an anti-FLAG tag Fab fragment by Roosild et al.⁽²⁰⁾, scFv and Fab fragments have been developed that recognize the hexapeptide sequence EYMPME (EE).^(17, 18) As outlined in Pai et al.⁽¹⁶⁾, the EE tag was theorized as a possible co-crystallization peptide for several reasons. First, it is a short peptide which is easier to mutate into a membrane protein loop than a long peptide sequence. Second, the sequence contains a tyrosine residue which are important amino acids in antibody-protein interactions through hydrogen bonding and hydrophobic interactions. Third, the two glutamate residues are available for electrostatic interactions, and the proline residue will decrease the conformational heterogeneity of the hexapeptide sequence. Lastly, the EE tag was chosen because of its established use in immunohistochemistry with commercial antibodies already available. In this study, these anti-EE scFv and Fab antibody fragments are used for the co-crystallization of the *E. coli* outer membrane protein intimin. This chapter details the expression, purification, and crystallization of each anti-EE antibody fragment, and introduces their unique ability to act as crystallization chaperones.

Experimental

ScFv/EE & Fab/EE Plasmids

The 3D5 scFv, developed by Kaufmann et al.⁽²¹⁾, was chosen as a good parent for the scFv/EE variants because of its large solvent cavity (75Å) that could potentially accommodate a membrane protein with the CDR regions free of crystal contact formation.⁽¹⁶⁾ The CDR regions of the 3D5 scFv were converted to hexahistidine (His₆) and EYMPME (EE) specificity with the gene cloned into the pAK400 vector by Pai et al.⁽¹⁶⁾ These scFv variants are referred to as scFv/His and scFv/EE respectively. By SDM, rational mutagenesis was performed on the scFv/EE protein to generate second generation scFv/EE proteins referred to as scFv/EE.k and scFv/EE.a.⁽¹⁷⁾ The scFv/EE.k protein contains the heavy chain mutations S30T and S32K. The scFv/EE.a protein contains the heavy chain mutations S30T and S32A.⁽¹⁷⁾ Second generation ScFv/EE variant genes were in the pAK400 vector with Chloramphenicol (CAM) selection. All scFv variants contain a C-terminal hexahistidine tag and N-terminal periplasmic leader sequences. The scFv/EE protein was converted to Fab format (Fab/EE) as outlined in Johnson et al.⁽¹⁸⁾ Fab/EE contains N-terminal periplasmic leader sequences, and two C-terminal peptide tags. A decahistidine tag is located on the light chain, and a FLAG tag is located on the heavy chain. The light and heavy chains of Fab/EE were cloned into the pFab vector with Ampicillin (AMP) selection.

Expression of scFv/EE Variants

The scFv/EE plasmid was transformed into *E. coli* C43 cells and plated onto CAM selective Luria broth (LB) agar plates (34µg/mL CAM). Starter cultures were prepared in which 6-8 culture tubes containing 5mL of selective LB media and 1 bacterial

colony were incubated for 6-8 hours at 225 RPM and 37°C. Each starter culture was inoculated into 1L of selective Terrific Broth (TB) media and incubated at 37°C, 225 RPM for 16-18 hours. Cells were centrifuged and resuspended into fresh selective TB media and inoculated into fresh 1L selective TB media. After shaking at 25°C, 225 RPM, for 1 hour, cells were induced with 1mM isopropyl- β -D-1-thiogalactopyranoside (IPTG) and continued shaking at 25°C for 5 hours. Cells were harvested by centrifugation, flash-frozen with liquid nitrogen, and stored at -80°C.

Purification of scFv/EE Variants

Buffers:

Lysis Buffer: 0.1M Tris pH 8.0, 0.75M Sucrose

EDTA Buffer: 1mM EDTA pH 8.0

Buffer A: 20mM Tris pH 8.0, 500mM NaCl, 20mM Imidazole

Buffer B: 20mM Tris pH 8.0, 500mM NaCl, 500mM Imidazole

GF Buffer (HBS): 50mM HEPES pH 7.5, 150mM NaCl

For every 4g of cells, re-suspension of the cell pellet occurred in 40mL of Lysis Buffer. Because the scFv is expressed in the periplasm, cells were lysed with lysozyme (10 mg of lysozyme in 1mL of Lysis Buffer for every 4g of cells). Upon addition of the lysozyme, 1mM ethylenediaminetetraacetic acid (EDTA) was added to the cell lysate solution (30mL per 4g cells). To 40mL oakridge tubes, 30mL of cell lysate was added, rocked at 4°C for 1 hour, stabilized with 500 μ L of 0.5M MgCl₂, and rocked for an additional 1 hour. The cell debris was pelleted via centrifugation at 25000 xg and the supernatant collected. The supernatant was added to snake skin dialysis tubing and dialyzed in 2L Buffer A for 2 hours, and transferred to another 2L of Buffer A for

overnight dialysis. The dialyzed sample was obtained and the protein (with C-terminal His₆ tag) purified by nickel affinity chromatography (Buffer A and Buffer B) with the elution peaks collected and buffer exchanged into GF buffer [HEPES Buffered Saline (HBS)]. Buffer exchanged protein was concentrated in Amicon MWCO 10K filters.

Expression of Fab/EE

The Fab/EE plasmid was transformed into *E. coli* C43 cells and plated onto AMP selective LB agar plates (60µg/mL AMP). Starter cultures were prepared in which 6-8 culture tubes containing 5mL of selective LB media and 1 bacterial colony were incubated for 6-8 hours at 225 RPM and 37°C. Each starter culture was inoculated into 1L of selective TB media and incubated at 37°C, 225 RPM for 16-18 hours. Cells were centrifuged and resuspended into fresh selective TB media and inoculated into fresh 1L selective TB media. After shaking at 25°C, 225 RPM, for 1 hour, cells were induced with 1mM IPTG and continued shaking at 25°C for 5 hours. Cells were harvested by centrifugation, flash-frozen with liquid nitrogen, and stored at -80°C.

Purification of Fab/EE

Lysis Buffer: 0.1M Tris pH 8.0, 0.75M Sucrose

EDTA Buffer: 1mM EDTA pH 8.0

Buffer A: 20mM Tris pH 8.0, 500mM NaCl, 20mM Imidazole

Buffer B: 20mM Tris pH 8.0, 500mM NaCl, 500mM Imidazole

GF Buffer: 50mM Tris pH 7.5, 200mM NaCl, 0.01% NaN₃

For every 4g of cells, re-suspension of the cell pellet occurred in 40mL of Lysis Buffer. Because the Fab fragments are expressed in the periplasm, cells were lysed with lysozyme (10 mg of lysozyme in 1mL of Lysis Buffer for every 4g of cells). Upon

addition of the lysozyme, 1mM EDTA was added to the cell lysate solution (30mL per 4g cells). To 40mL oakridge tubes, 30mL of cell lysate was added, rocked at 4°C for 1 hour, stabilized with 500µL of 0.5M MgCl₂, and rocked for an additional 1 hour. The cell debris was pelleted via centrifugation at 25000 xg and the supernatant collected. The supernatant was added to snake skin dialysis tubing and dialyzed in 2L Buffer A for 2 hours, and transferred to another 2L of Buffer A for overnight dialysis. The dialyzed sample was obtained and the protein (with C-terminal His₁₀ tag) purified by batch purification [manual nickel affinity chromatography (Buffer A and Buffer B)] with the Buffer B elution sample collected and ran over a Sup75 column for gel filtration into GF buffer. Gel filtration fractions were concentrated in Amicon MWCO 10K filters.

Results & Discussion

scFv/EE and Fab/EE Antibody Fragments

The first and second generation scFv/EE antibody fragments and the Fab/EE fragment are stable, hypercrystallizable proteins. Their biophysical characteristics were enhanced during the development process making these antibody fragments ideal co-crystallization chaperones.^(17, 18) It has been shown that scFv/EE variants and Fab/EE fragments have nano-molar affinity for internal EE tags indicating that a tight complex will form between the antibody fragment and the EE-tagged membrane protein.

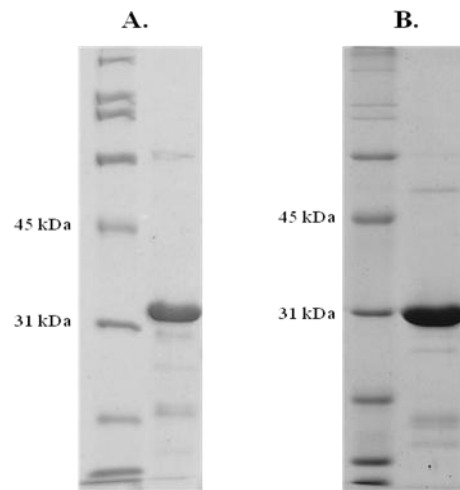


Figure 2.1. ScFv/EE.k and Fab/EE SDS-PAGE
A. SDS-PAGE of GF purified scFv/EE.k in HBS
B. SDS-PAGE of GF purified Fab/EE in GF Buffer

The fragments are easily expressed through standard recombination techniques in *E. coli*. After gel filtration purification, the proteins have a purity >95% and are in high protein yield. A 12% resolving SDS-PAGE gel of a scFv/EE fragment and the Fab/EE fragment after gel filtration are shown in Figure 2.1. A scFv/EE.k nickel affinity and Fab/EE Sup75 chromatogram are shown in Appendix A Figure A.1. Representative protein yields for all scFv variants and Fab/EE are shown in Appendix A Table A.1.

Crystallization trials for scFv/His were performed by Sibel Kalyoncu. The structure of ScFv/His (8mg/mL in HBS) was solved with crystals grown at room temperature using sitting drop vapor diffusion. The condition contained 0.2M KI, 0.001M Guanidinium HCl, and 18% (w/v) PEG 8000.⁽¹⁷⁾ Alongside Sibel, initial crystallization trials for scFv/EE.k were identified both from sparse matrix screening and optimization of conditions for the first generation scFv/EE. Crystallization variables that were optimized included protein concentration, temperature, and mother liquor contents. Ultimately, the structure of scFv/EE.k (7.5 mg/mL in HBS) was solved with crystals grown at 4°C using sitting drop vapor diffusion. The condition contained 0.1M Tris pH 8.5, 0.2M Li₂(SO₄)₂, 3% 6-aminohexanoic acid, and 24% (w/v) PEG 8000.⁽¹⁷⁾ Crystals grew to a size of 30-40µm within 2 weeks.⁽¹⁷⁾ For the scFv/EE.a variant, initial crystallization trials were identified both from sparse matrix screening and optimization of conditions for the first generation scFv/EE. Crystallization variables that were optimized included protein concentration, temperature, and mother liquor contents. The structure of scFv/EE.a (7.5 mg/mL in HBS) was solved with crystals grown at 4°C using sitting drop vapor diffusion. The condition contained 0.1M BisTris pH 6.5, 0.2M

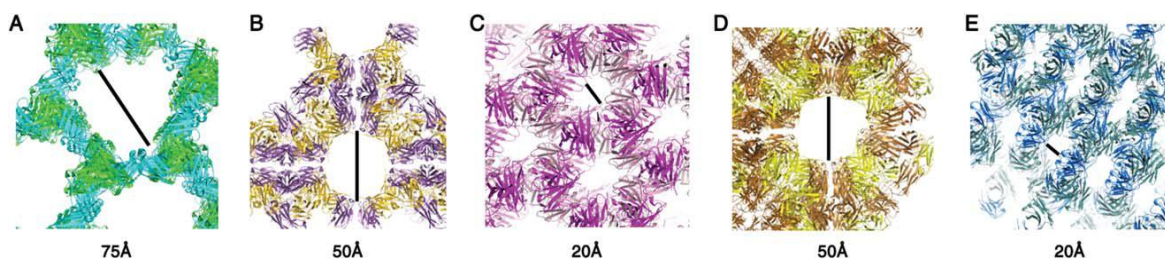


Figure 2.2. Engineered Single Chain Antibody Fragment Crystal Lattices

Crystal lattices of the scFv variants. Solvent channel diameter is indicated below each subfigure and a black line. Figure as shown in Kalyoncu et al.⁽¹⁷⁾

A. 3D5 scFv B. scFv/EE C. scFv/His D. scFv/EE.a E. scFv/EE.k

Mg(OAc)₂, and 21% (w/v) PEG 8000.⁽¹⁷⁾ Crystals grew to a size of 20-30µm within 3-4 weeks.⁽¹⁷⁾ All data collection [Southeast Regional Collaborative Access Team (SER-CAT) beamline 22-ID at the Advanced Photon Source at Argonne National Laboratory] and data refinement (HKL2000 and Coot) was performed by Sibel.

The crystal lattice of 3D5 is shown in Figure 2.2.A, with the crystal lattice of scFv/EE and scFv/His shown in Figure 2.2.B and Figure 2.2.C. However, both scFv/His and scFv/EE showed significant reduction in the size of the solvent cavity, and the CDR regions were involved in crystal contact formation.^(16, 17) Through rational mutagenesis, two second generation scFv/EE antibody fragments were created (scFv/EE.k and scFv/EE.a) in hopes of restoring the original 3D5 crystal lattice.⁽¹⁷⁾ The crystal lattices of scFv/EE.a and scFv/EE.k are shown in Figure 2.2.D and Figure 2.2.E. Unfortunately, both second generation scFv/EE's crystallized in different crystal lattices. Even though the 3D5 crystal lattice could not be obtained for our engineered scFv/EE variants, each scFv/EE variant could still be used as co-crystallization chaperones since the crystal lattice will almost inevitably change once complexed to a membrane protein.

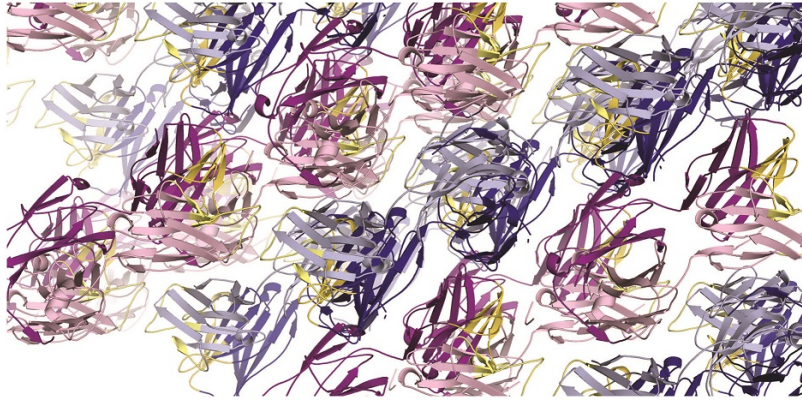


Figure 2.3. Engineered Fab Fragment Crystal Lattice

Crystal lattice of the Fab/EE antibody fragment. Light colors correspond to light chain regions, while the darker counterparts correspond to heavy chain regions. Yellow highlights the CDR of each monomer. Figure as shown in Johnson et al ⁽¹⁸⁾.

Crystallization trials of Fab/EE were performed by Jennifer Johnson. The structure of Fab/EE (6.5 mg/mL in HBS) was solved from crystals grown at room temperature using sitting drop vapor diffusion. The condition contained 0.1M HEPES pH 7.5, 0.1M Ca(OAc)₂, 3% 1-propanol, and 20-26% (w/v) PEG 8000.⁽¹⁸⁾ The crystal lattice of Fab/EE is shown in Figure 2.3.

It may be asked as to why only a first generation scFv/His was created. Binding of the scFv/His to a hexa-histidine tag is pH dependent. In order for the general use of co-crystallization chaperones, variables such as pH should be independent of complex formation. Second generation scFv/EE variants (scFv/EE.a and scFv/EE.k) have enhanced biophysical characteristics compared with the parent scFv/EE. ScFv/EE.k and scFv/EE.a displayed an increase in monomeric protein, higher melting temperatures, and increased affinity for the EE tag compared with scFv/EE.⁽¹⁷⁾ Fab/EE engineering resulted in a protein with increased expression level, a higher melting temperature, and an increased amount of monomeric protein compared with the parent scFv/EE.⁽¹⁸⁾

Even though both scFv/EE and Fab/EE fragments can be used as co-crystallization chaperones, the Fab/EE fragment has several advantages for its use as a chaperone. First, the Fab/EE fragment does not form a dimer in solution as can be observed for the scFv/EE variants after gel filtration (Appendix A Figure A.2). Second, the Fab fragment can reach a higher protein concentration (~8 mg/mL) compared to the scFv/EE fragments (~6.5-7 mg/mL). Third, the Fab fragment is nearly double the size of the scFv fragment (54.3 kDa compared to 28.0 kDa) which can correlate to more surface area available for strong crystal contacts being formed in the nucleation of an antibody fragment-membrane protein complex.

Combining their enhanced biophysical characteristics and their easy expression and purification, the scFv/EE variants and the Fab/EE fragment are ideal high-throughput chaperones for membrane proteins. As a proof-of-concept for these novel antibody fragments, both scFv/EE and Fab/EE fragments will be complexed with the membrane protein intimin followed by co-crystallization trials. If an intimin-antibody fragment complex structure can be solved, it would provide strong evidence for the use of the engineered, hypercrystallizable antibody fragments as membrane protein crystallization chaperones.

CHAPTER 3

PROTEIN ENGINEERING, EXPRESSION, AND PURIFICATION OF THE INTIMIN VARIANTS

Abstract

In order for the co-crystallization of the scFv/EE or Fab/EE fragment with the membrane protein intimin to occur, the EE tag needed to be inserted into the intimin protein. A total of 5 intimin-EE variants were constructed by SDM, with each variant containing one EE tag in a different extramembranous location. These individual variants are known as intimin-EE1, intimin-EE3, intimin-EE4, intimin-EE7, and intimin-EE8. The variants intimin-EE1 and intimin-EE3 contain the EE tag in the periplasmic α -helix region. Intimin-EE4 contains the EE tag in the L5 extracellular loop region. Intimin-EE7 and intimin-EE8 have the EE tag in the same location within the L4 extracellular loop with intimin-EE8 containing a two alanine extender sequence on either side of the EE tag. Even though SDM was successful for all 5 intimin-EE variants, intimin-EE4 was not expressed as shown by Western blotting, and intimin-EE3 could not be purified via nickel affinity chromatography. Intimin-EE1 could be successfully purified, but the final yield was substantially lower than the intimin-EE7 and intimin-EE8 final yields.

Introduction

Intimin is an outer membrane protein found in pathogenic bacteria such as *E. coli*. The function of intimin is to aid in the attachment of the *E. coli* bacterium to epithelial cell linings of the intestinal tract through the translocated intimin receptor (Tir).⁽¹⁹⁾ The tertiary structure of the WT intimin protein includes a β -domain (β -barrel) that spans the outer membrane, and 4 passenger domains that extend into the extracellular space and are

connected by a flexible linker that spans the inside of the β -barrel. The protein structure of the β -barrel was solved by Fairman *et al.*⁽¹⁹⁾ It is composed of 12 anti-parallel β -sheets and a periplasmic α -helix. For the purposes of this study, only the β -barrel construct was considered for complexation with an antibody fragment. The intimin β -barrel was chosen as the test membrane protein for co-crystallization with the engineered antibody fragments for several reasons. First, intimin was chosen because of its supposed ease of crystallization (by membrane protein standards). Intimin β -barrel crystals were previously grown in crystallization conditions containing detergent, detergent bicelles, and lipidic cubic phases.⁽¹⁹⁾ A membrane protein with supposed crystallization flexibility was deemed a positive asset for this proof-of-concept project. To try and show the versatility of this co-crystallization method, both β -barrel (intimin) and α -helical membrane proteins (Signal Peptide Peptidase, project not discussed) are being tested for co-crystallization with the engineered antibody fragments. This chapter details the protein engineering, expression, and purification of the intimin-EE proteins.

Experimental

Intimin Plasmid

The WT intimin pET9 plasmid with kanamycin (KAN) selectivity was generously provided by Dr. Susan K. Buchanan (NIH). The intimin gene encoded for residues 208-449 from *E. coli* O157:H7 which corresponded to the intimin β -barrel with the associated periplasmic α -helix.⁽¹⁹⁾ The gene encoded for an N-terminal PelB leader sequence along with a N-terminal decahistidine tag with associated TEV cleavage site (10xHis-TEV-Int₂₀₈₋₄₄₉).⁽¹⁹⁾

Intimin-EE Protein Engineering

The intimin-EE variants were generated by SDM of the pET9 intimin construct with oligonucleotides containing point mutations for the EE tag. Mutant pET9 vectors (intimin-EE plasmids) were obtained after plasmid isolation by miniprep and their sequences confirmed by MWG Operon sequencing service. The QuikChange Lightning Site-Directed Mutagenesis Kit (with the included protocol) produced by Agilent Technologies was used for all SDM experiments. The oligonucleotide primers were ordered and obtained from MWG Operon. The sense and antisense oligonucleotide sequences are documented in Appendix B Table B.1.

Expression of the Intimin Variants

The intimin-EE plasmid was transformed into *E. coli* BL21 (DE3) cells and plated onto KAN selective LB agar plates (50µg/mL KAN). Several colonies were selected and inoculated in 10mL of selective LB broth and shaken at 220 RPM at 37°C until OD₆₀₀ reached 0.6. Glycerol stocks (500µL OD₆₀₀ = 0.6 bacteria culture, 500µL of LB media, 50% glycerol) were prepared, flash-freezed in liquid nitrogen, and stored at -80°C.

To screen for intimin protein expression, a glycerol stock from each colony was added to 30mL of selective TB media and shaken at 220 RPM at 20°C until OD₆₀₀ was between 10 and 15. For each cell growth medium, 3x10⁸ cells were harvested and 100µL of 4X SDS-PAGE running buffer added. The cells were thermally lysed at 95°C for 10 minutes. A SDS-PAGE and western blot analysis was performed on each colony. For each intimin variant, the best colony (highest expression of intimin protein) was selected for large scale growth and protein purification.

For large scale growth of each intimin variant, a glycerol stock from a colony that expressed the protein was thawed and 6-8 starter cultures prepared in selective LB media (5mL each). Starter cultures were shaken at 220 RPM at 37°C for 6-8 hours. To a flask containing 500mL of selective TB media, 1 starter culture was added and cells were shaken at 220 RPM at 20°C for 48-72 hours. The cells were harvested, flash-frozen with liquid nitrogen, and stored at -80°C.

Purification of the Intimin Variants

Buffers:

Buffer A: 50mM Tris pH 8.0, 200mM NaCl, 10% glycerol, 0.1% DDM

Buffer B: 50mM Tris pH 8.0, 200mM NaCl, 250mM Imidazole, 10% glycerol, 0.1% DDM

Buffer E: 50mM Tris pH 7.5, 200mM NaCl, 0.01% NaN₃, 0.05% DDM (LDAO)

Lysis Buffer: 50mM TRIS pH 7.50, 200 mM NaCl, 10 mM MgCl₂, 5 µg/ml DNase I, 50 µg/ml, AEBSF protease inhibitor

Solubilization Buffer: 50mM TRIS pH 8.0, 200 mM NaCl, 20 mM imidazole, 5% Eluent

For each purification cycle, 20g of cell paste was collected and re-suspended in 100mL of Lysis Buffer. Cells were cracked using the French Press method (1200 psi, every 25mL cracked twice). The membranes were then harvested by ultra-centrifugation by spinning at 118000 xg for 1 hour. For every cell lysis cycle, half of the membranes were flash-frozen in liquid nitrogen and stored at -80°C.

Roughly 3-4g of isolated membranes were re-suspended into solubilization buffer using a dounce homogenizer. Resuspended membranes were allowed to stir overnight

(16-18 hours) at 4°C. The supernatant containing the eluent solubilized intimin protein was collected by ultra centrifugation at 118000 xg for 1 hour. The supernatant was purified by Nickel Affinity Chromatography (Ni-NTA) using Buffers A and Buffer B. The Ni-NTA elution fractions were concentrated in an Amicon MWCO 10K or 30K filter and loaded onto a Sephacryl 300 or Superose 12 10/300 GL column for gel filtration (GF) using Buffer E. The GF elution fractions were concentrated in an Amicon MWCO 10K or 30K filter.

Results & Discussion

Intimin-EE Protein Engineering

For complexation and co-crystallization with the scFv/EE and Fab/EE antibody fragments, a total of 5 intimin-EE variants were constructed. The 5 intimin-EE variants are known as intimin-EE1, intimin-EE3, intimin-EE4, intimin-EE7, and intimin-EE8. Intimin-EE 1 and intimin-EE3 contain the EE tag within the periplasmic α -helix. Intimin-EE4 contains the EE tag within the L5 extracellular loop. Intimin-EE7 and Intimin-EE8 contain the EE tag in the same location of the L4 extracellular loop; however, intimin-EE8 contains a two-alanine extender sequence on both sides of the EE tag. The rationale for the alanine extender sequence was to increase the accessibility of the EE tag to the CDR regions of the scFv or Fab anti-EE antibody fragments. Accessibility was deemed an issue because of failed complexation experiments with all other intimin-EE variants when solubilized in LDAO (discussed in chapter 4). The physical location of each EE tag is shown in Figure 3.1.

Initial SDM trials for all the intimin-EE variants were successful except for intimin-EE1. A second round of SDM for intimin-EE1 was successful upon addition of

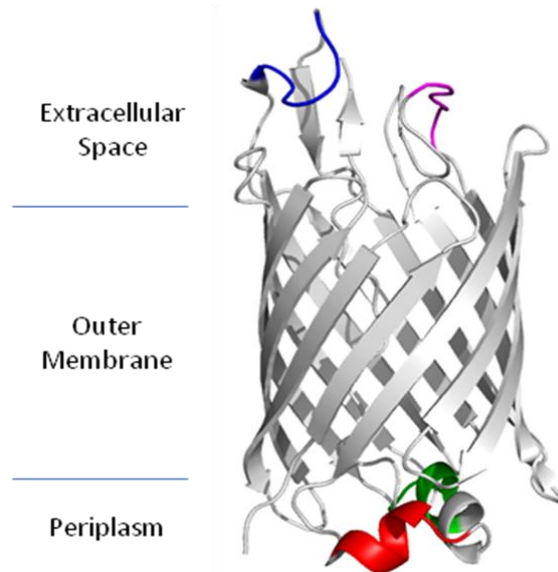


Figure 3.1. Intimin-EE Variants

Pymol cartoon representation of the intimin protein β -barrel tertiary structure. The different locations of the EE tag are displayed. Each intimin-EE variant is as follows: intimin-EE1 (red, α -helix), intimin-EE3 (green, α -helix), intimin-EE4 (purple, L5 loop), intimin-EE7 (blue, L4 loop), intimin-EE8 (blue, L4 loop, alanine extender sequences not shown).

2% dimethyl sulfoxide (DMSO) to the SDM mixture. Intimin-EE8 was generated by Ivan Morales during the intimin-EE1 SDM trials. The selection of these 5 intimin-EE variants among hypothesized others relied upon the biophysical properties of the oligonucleotide primers, and the locations of the EE tag within the tertiary structure of the protein. It was important for the EE tag to be placed in a location that was not only accessible to an antibody fragment, but also would not disrupt the correct folding of the intimin β -barrel. Locations that seemed accessible and not to cause folding interference were the extracellular loop regions and the periplasmic α -helix. Fairman et al. had shown through heat-modifiable mobility assays with intimin α -helix truncation variants that the α -helix was not required for proper folding of the β -barrel.⁽¹⁹⁾ The oligonucleotide selection criteria included the least amount of mutations necessary for the insertion of the

EE tag, optimal primer length (<100 bp), no predicted secondary structure of the primers or primer dimers, and high melting temperatures ($T_m > 78^\circ\text{C}$). The sense and antisense primers for intimin-EE1 contained strong secondary structure but no primer dimers were predicted. The primer length was 78 bp with a predicted T_m of 89.52°C . The primers for intimin-EE3 contained strong secondary structure but no primer dimers were predicted. The primer length was 87 bp with a predicted T_m of 92.39°C . Strong secondary structure was predicted for the intimin-EE4 primers with no primer dimers. The intimin-EE4 primer length was 75 bp long with a predicted T_m of 92.43°C . The primers for intimin-EE7 were not predicted to form primer dimers, but had strong secondary structure. The intimin-EE7 primer length was 84 bp with a T_m of 93.85°C . Intimin-EE8 primers were predicted to have very strong secondary structure in which >2% DMSO was added to the SDM mixture as reported by Mr. Morales. The primer lengths were 85 bp long with a predicted T_m of 99.35°C .

Expression and Purification of the Intimin Variants

To test the expression level of each intimin-EE variant, SDS-PAGE analysis followed by Western Blot analysis was performed on heat lysed cell colonies. Western blot analysis revealed expression of intimin-EE3 and intimin-EE7 within each colony chosen, but showed that intimin-EE4 failed to be expressed. The western blot for intimin-EE3, intimin-EE4, and intimin-EE7 is shown in Appendix B Figure B.2. The western blot for intimin-EE1 failed; however, the SDS-PAGE revealed intimin-EE1 expression in two of the four colonies chosen. The SDS-PAGE for intimin-EE1 is shown in Appendix B Figure B.2. The intimin-EE8 western plot was successful and performed by Mr. Morales (not shown).

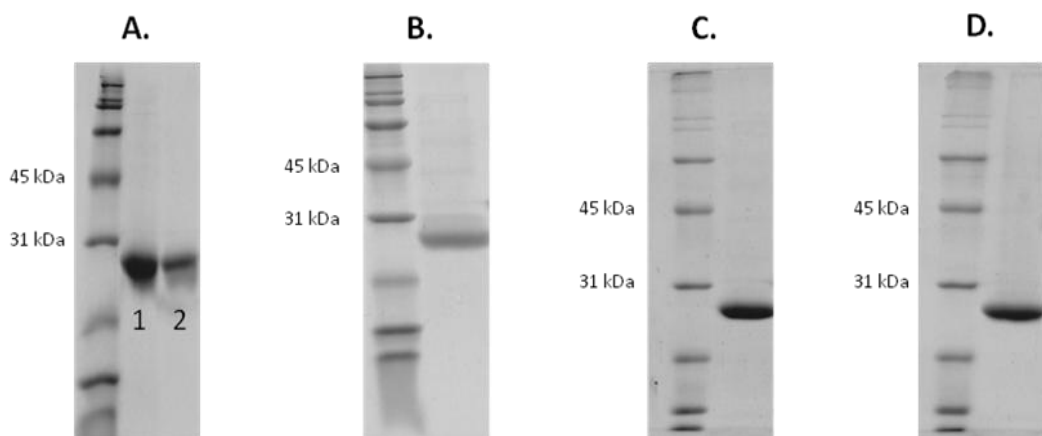


Figure 3.2. Intimin-EE Variants SDS-PAGE Gels

- A. SDS-PAGE of WT intimin after S12 gel filtration. Lane 1 contains LDAO solubilized WT intimin. Lane 2 contains DDM solubilized WT intimin.
- B. SDS-PAGE of intimin-EE1 solubilized in LDAO detergent after S300 gel filtration.
- C. SDS-PAGE of intimin-EE7 solubilized in DDM detergent after S12 gel filtration.
- D. SDS-PAGE if intimin-EE8 solubilized in DDM detergent after S12 gel filtration.

Intimin-EE1, intimin-EE7, and intimin-EE8 could all be purified by nickel affinity chromatography followed by gel filtration. Initial gel filtration purifications utilized the Sephacryl 300 (S300) column; however, it was replaced by the Superose 12 (S12) column for all later gel filtrations due to its smaller column volume and higher resolution. The S12 runs were run in duplicate to minimize the loss of protein due to the necessity of smaller injection volumes. Only one of the S12 gel filtration runs are shown in Appendix B Figure B.3. After gel filtration, the intimin variants are >95% pure as can be shown by the 12% resolving SDS-PAGE gels shown in Figure 3.2. Intimin-EE3 failed to be isolated by nickel affinity chromatography. Therefore, from both the expression and purification trials, only three of the five intimin-EE variants could be isolated for potential complexation and crystallization trials with scFv/EE or Fab/EE. Of the three intimin-EE variants, intimin-EE7 and intimin-EE8 resulted in the highest yield per gram

of membrane when isolated in both Lauryldimethylamine-N-oxide (LDAO) and n-dodecyl- β -D-maltopyranoside (DDM) detergent. Nickel Affinity and S12 gel filtration chromatograms for intimin-EE1, intimin-EE3, intimin-EE7, and intimin-EE8 can be found in Appendix B Figure B.3. Relative yields of all the intimin variants in LDAO and DDM detergents can be found in Appendix B Table B.2 and Table B.3.

CHAPTER 4

COMPLEXATION OF THE INTIMIN-EE VARIANTS WITH THE SCFV/EE AND FAB/EE ANTIBODY FRAGMENTS

Abstract

Before co-crystallization trials could begin, complex formation of intimin-EE with scFv/EE variants and with Fab/EE had to be shown to occur in aqueous solution. The experimental design for observing such a complexation event was gel filtration followed by SDS-PAGE analysis. Initial complexation trials of LDAO solubilized intimin-EE variants with scFv/EE variants and Fab/EE were unsuccessful. The solubilization detergent was changed to DDM which resulted in observable complex formation for scFv/EE and Fab/EE, but not enough to condone co-crystallization trials. The complex mixture was expected to obey Le Chatelier's Principle, so constituent protein concentrations were increased and length of GF elution was decreased. Complex formation increased for both scFv/EE variant and Fab/EE complexes. In conclusion, complexation of intimin-EE with scFv/EE variants and Fab/EE was observed, yet optimization of variables such as detergent identity and initial protein concentrations were found to be critical for this EE complex interaction.

Introduction

Before crystallization trials of any protein or protein complex can begin, the biophysical characteristics and biophysical limitations of the macromolecule in aqueous solution must be understood. Such biophysical properties include, but not limited to, solubility limits, temperature sensitivities, and binding affinities. In the case for intimin and the engineered antibody fragments, the biophysical properties of each individual

protein had been explored and are well documented.^(16,17,18,19) However, biophysical complexation characteristics of the intimin-EE protein with the anti-EE antibody fragments had to be explored before co-crystallization trials could begin. Principally, the complexation of intimin-EE with the anti-EE antibody fragments had to be shown to occur in aqueous solution. The following chapter documents the experimental procedures and results obtained that led to the conclusion of the EE complex being formed, along with complexation variables that must be optimized for a complex to be observed.

Experimental

Intimin-EE & scFv/EE Complex Formation

To form the intimin-EE & scFv/EE complex, 200µg of intimin-EE variant solubilized in either LDAO or DDM detergent was mixed in a 1:1 molar ratio with the purified scFv/EE variant. The sample was completed to 1 mL, incubated on ice for 3 hours and then loaded onto a S300 column for gel filtration (column volume 120mL). Gel filtration of S300 samples occurred on AKTA FPLC, AKTA Purifier, or AKTA PURE purification platforms. If the sample was to be loaded onto a S12 column (column volume 24mL), the 1:1 mixture was first completed to 250µL and then incubated on ice for 3 hours. Gel filtration of S12 samples occurred on the AKTA PURE purification platform. The elution fractions were collected, concentrated in an Amicon MWCO 10K filter, and mixed in a 1:1 volume ratio with 2X laemili. The laemili fractions were loaded and ran on a 12% resolving SDS-PAGE gel.

Intimin-EE & Fab/EE Complex Formation

To form the intimin-EE & Fab/EE complex, the proteins were mixed in a 1:1 molar ratio with the final concentration of the Fab/EE being 4 mg/mL in 250µL. The

mixture was incubated on ice for 2 hours and then loaded onto a S12 column for gel filtration. Gel filtration of S12 samples occurred on the AKTA PURE purification platform. The elution fractions were collected, concentrated in an Amicon MWCO 10K filter, and mixed in a 1:1 volume ratio with 2X laemili. The laemili fractions were loaded and ran on a 12% resolving SDS-PAGE gel.

Results & Discussion

Complexation of Intimin-EE & scFv/EE variants

The experimental design for observing the complex formation of intimin-EE with the scFv/EE variants (scFv/EE and scFv/EE.k) included gel filtration followed by SDS-PAGE analysis. Because the hypothesized outcome would be the scFv recognizing the EE tag within the intimin protein, it would be expected to see a single elution peak in the gel filtration chromatogram. Furthermore, the intimin-EE & scFv/EE.k complex would elute at a smaller volume (faster elution) than either of its individual constituents since the complex has a greater mass. If each elution fraction were to be collected and ran on a SDS-PAGE gel, it would be expected to see both proteins within each fraction with approximately equal band intensity. As the negative control, gel filtration and SDS-PAGE analysis of WT intimin with scFv/EE.k should reveal separate elution of the proteins. As detailed by Fairman et al., gel filtration of WT intimin occurred in LDAO detergent with a gel filtration column volume of 120 mL.⁽¹⁹⁾ Therefore, to begin complexation experiments of intimin-EE with scFv/EE.k, intimin was solubilized in LDAO detergent and gel filtration was performed on the S300 column.

To observe which intimin-EE variant would have the highest binding affinity for scFv/EE.k, LDAO solubilized intimin-EE7, intimin-EE8, and intimin-EE1 all entered

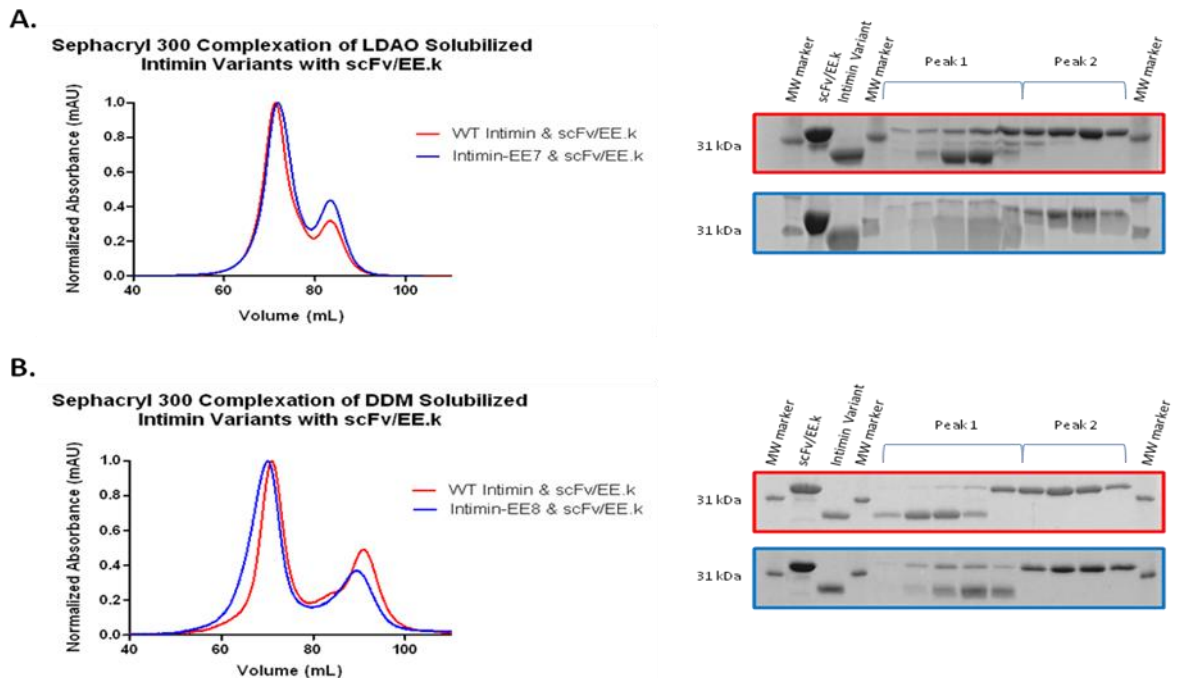


Figure 4.1. Intimin-EE and scFv/EE.k S300 Complexations

- Comparison of S300 gel filtration and SDS-PAGE analysis of LDAO solubilized intimin-EE7 & scFv/EE.k (blue) with the negative control of WT intimin & scFv/EE.k (red). Chromatogram colors are coordinated with their respective gel. Elution fractions of peak 1 for both experiments seem identical; therefore complexation does not occur in LDAO detergent. Peak 1 and peak 2 corresponds to ~70mL and ~85mL elution volumes respectively.
- Comparison of S300 gel filtration and SDS-PAGE analysis of DDM solubilized intimin-EE8 & scFv/EE.k (blue) with the negative control of WT intimin & scFv/EE.k (red). Chromatogram colors are coordinated with their respective gel. Negative control shows separate elution of WT intimin and scFv/EE.k compared with the co-elution of intimin-EE8 and scFv/EE.k. Peak 1 and peak 2 corresponds to ~70mL and ~85mL elution volumes respectively.

complexation trials. Interestingly, gel filtration followed by SDS-PAGE analysis revealed that the intimin-EE & scFv/EE.k complex was not formed for any of the intimin-EE variants. Two elution peaks were observed for each gel filtration run which SDS-PAGE analysis revealed to be separate elution of the intimin-EE protein and scFv/EE.k. To ensure that complex formation was not being hindered due to the identity of the scFv, complexation was tested with the first generation scFv/EE. However, separate elution of the intimin-EE protein and scFv/EE was evident from gel filtration which was confirmed

by SDS-PAGE analysis. Due to the number of complexation experiments performed with LDAO solubilized intimin variants, only a representative gel filtration and SDS-PAGE analysis is shown for intimin-EE7 & scFv/EE.k with the negative control in Figure 4.1.A. However, Appendix C Table C.1 records each complexation experiment performed for LDAO solubilized intimin variants with the scFv/EE and scFv/EE.k antibody fragments. Because scFv identity was not effecting the formation of the intimin-EE & scFv complex, it was hypothesized that the LDAO detergent was interfering in complex formation. Superose 12 detergent screens were performed in which the LDAO detergent in the gel filtration buffer was exchanged for DDM and Fos-Choline-12 (FC-12) detergents. The gel filtration and SDS-PAGE analyses of the detergent screens revealed the intimin protein to be stable in both DDM and FC-12 detergents (data not shown). For the complexation experiments, DDM was the detergent choice based on its lower critical micelle concentration (CMC) and history of use as a complexation detergent in the lab. DDM solubilized intimin-EE7 and intimin-EE8 were mixed with scFv/EE.k and the mixture ran over the S300 column. Upon first inspection, the results seemed identical to the LDAO solubilized results. However, SDS-PAGE comparison of the intimin-EE7 and intimin-EE8 complexation with the negative control revealed a small amount of the complex was being formed. As shown in Figure 4.1.B, the DDM solubilized WT intimin & scFv/EE.k SDS-PAGE analysis revealed separate elution of the proteins with the exception of some possible elution overlapping of the individual proteins. The SDS-PAGE analysis of the intimin-EE7 and intimin-EE8 complexations revealed greater intensity of the scFv band co-eluting with the intimin protein.

When analyzing the S300 data (implying that this does not apply to S12 data that will be presented later), it should be noted that the intensity of the bands between peak 1 and peak 2 cannot be compared. When concentrating each S300 fractions for SDS-PAGE analysis, each fraction was concentrated to the point that the absorbance would be 100 mAu to be consistent between different gel filtration experiments. For example, if peak 1 had an absorbance of 50 mAu and peak 2 had an absorbance of 25 mAu, peak 1 fractions were 2X concentrated and peak 2 fractions were 4X concentrated. Therefore, the greater intensity of peak 2 bands was not due to more scFv/EE variant present over intimin-EE, but was the error in fraction concentration. However, the presence or absence of scFv/EE variant co-eluting in peak 1 fractions can be analyzed which would reveal that the complex is forming in small amounts in S300 DDM samples.

Since it is known that the intimin-EE & scFv/EE variant complex will form when the intimin-EE protein is solubilized in DDM detergent, it was necessary to increase the amount of complex being formed for co-crystallization trials. It was hypothesized that the amount of complex being observed was an equilibrium mixture. Therefore if the concentrations of intimin-EE and the scFv/EE variants were increased, then by Le Chatelier's Principle the equilibrium would shift towards formation of the complex. It had already been shown by Mr. Morales who was working with the Fab/EE protein that binding was concentration dependant. In addition, it was suspected that the S300 elution length of 120mL was pulling the complex apart. Therefore, the same amount of intimin-EE protein (200µg) was mixed in a 1:1 molar ratio with scFv/EE.k, yet the total volume of the mixture was reduced to 250µL to increase the protein concentration and to meet S12 column injection volume requirements. The mixture was run over a S12 column

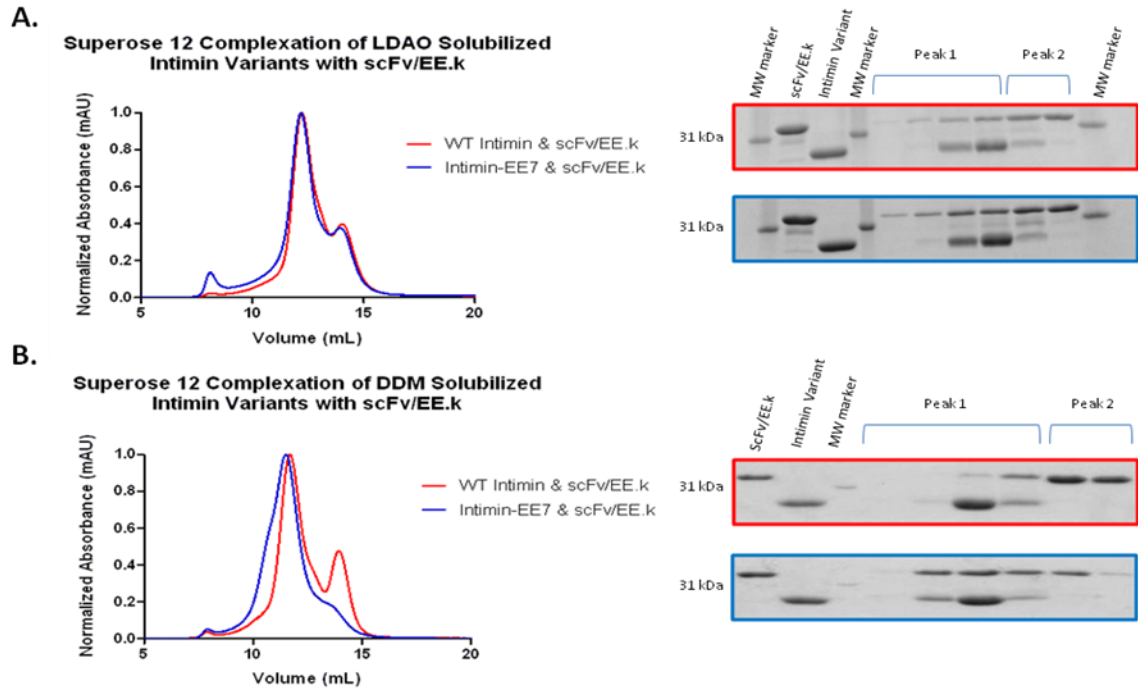


Figure 4.2. Intimin-EE and scFv/EE.k S12 Complexations

- A. Comparison of S12 gel filtration and SDS-PAGE analysis of LDAO solubilized intimin-EE7 & 3D5/EE_48.k with the negative control. Chromatogram colors are coordinated with their respective gel. The S12 chromatograms and SDS-PAGE analyses are nearly identical strongly suggesting no binding interaction between the scFv/EE variant and intimin-EE7. Peak 1 and peak 2 fractions corresponds to ~11mL and ~14mL elution volumes respectively
- B. Comparison of S12 gel filtration and SDS-PAGE analysis of DDM solubilized intimin-EE7 & 3D5/EE_48.k with the negative control. Chromatogram colors are coordinated with their respective gel. As compared with the negative control, peak 2 absorbance significantly decreased coupled with a shift in elution volume of peak 1. SDS-PAGE analysis reveals co-elution of proteins in peak 1 with similar band intensity. Therefore complexation occurs when intimin-EE is solubilized in DDM detergent. Peak 1 and peak 2 fractions corresponds to ~11mL and ~14mL elution volumes respectively.

which had a column volume of approximately 24 mL. The results of the DDM solubilized S12 runs are shown in Figure 4.2.B. As compared with the negative control, the mixture of intimin-EE7 with scFv/EE.k resulted in a slightly left shifted peak 1 with a smaller peak 2. SDS-PAGE analysis showed peak 1 to be the co-elution of intimin-EE7 and scFv/EE.k and smaller peak 2 to be uncomplexed scFv/EE.k. When comparing these results to the S300 DDM runs, there is significantly more complex formed providing

strong evidence for the equilibrium hypothesis to be correct. All S12 complexations are recorded in Appendix C Table C.2.

Although LDAO did not give promising results with S300 complexation, a last attempt to observe LDAO complex formation was performed with S12 gel filtration. At that point, it remained to be seen if LDAO solubilized intimin-EE would form a complex with scFv/EE.k if the concentrations of the individual proteins were increased. These results are shown in Figure 4.2.A. The S12 gel filtration revealed complex formation did not occur. There is no difference between the intimin-EE7 with scFv/EE.k run and the negative control. As a reminder, the S12 SDS-PAGE gels can be fully analyzed because the concentration error for the S300 runs was not propagated into the S12 experiments. Each S12 fraction was concentrated equally in an Amicon MWCO 10K filter followed by gel electrophoresis.

The complexation experiments of intimin-EE with the scFv/EE variants uncovered complexation variables that must be optimized in order for complex formation to occur. It was first found that complexation is critically dependant upon the identity of the detergent. Complexation did not occur in LDAO detergent, but the intimin-EE & scFv/EE variant complex was observed with DDM detergent. Why was this complexation dependancy observed? The molecular structures of LDAO and DDM are shown in Figure 4.3. Both detergents have a dodecyl tail for interaction with the hydrophobic β -barrel of intimin-EE. However, the hydrophilic heads of the detergents differ. LDAO has a zwitterionic head, while the hydrophilic end of DDM is a nonionic disaccharide. It is possible that the zwitterionic head of LDAO was creating an unfavorable ionic microenvironment around the EE tag that might hinder complex formation. This

structural analysis would also conclude that complex formation in FC-12 would probably not occur since FC-12 is also a charged detergent.

It is not too surprising that the complexation event is equilibrium driven. The

vast majority of chemical systems will reach equilibrium so long as there is not an external force keeping it from doing so. When the mixture was incubated on ice, there was no external force keeping the mixture from reaching equilibrium. Temperature trials were not performed because all purification steps including gel filtration were carried out at 4°C due to the temperature sensitivity of the proteins. Therefore, a system variable (concentration) was changed to force the equilibrium towards the complex. Yet there is another variable that is easily overlooked- the identity of the gel filtration column resin. The S300 column is composed of sephacryl resin, while the S12 column is composed of superose resin. In addition to reducing the elution volume from 120 mL to ~24 mL (S300 vs. S12), complexation could have been increased by the fact the resin was changed to superose.

A fact that must be addressed was that the intimin-EE and scFv/EE variant proteins were mixed in a 1:1 molar ratio. However, a single gel filtration elution peak

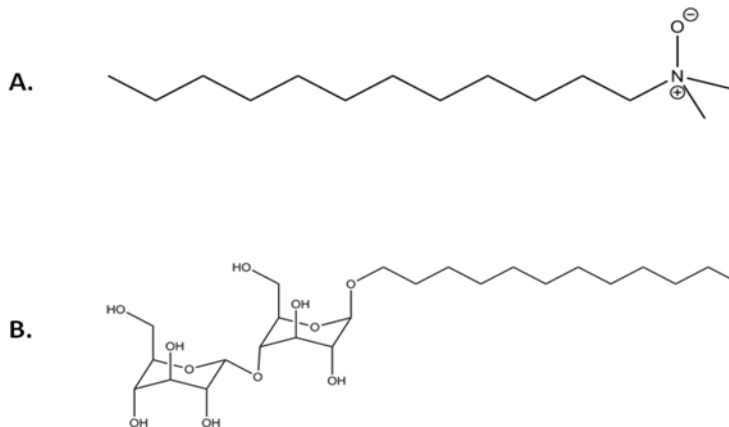


Figure 4.3. Detergent Chemical Structures

- A. Molecular structure of Lauryldimethylamine-N-oxide (LDAO) detergent
- B. Molecular structure of n-dodecyl-β-D-maltopyranoside (DDM) detergent.

was never observed. Even with the S12 gel filtration runs, a shoulder peak 2 was observed that was shown to be un-complexed scFv/EE.k. These results indicate that the intimin-EE & scFv/EE variant interaction may not be 1:1 or the real concentration of intimin-EE was not exactly measured due to possible interference of the detergent micelles.

Complexation of Intimin-EE & Fab/EE

Many of the complexation variables such as choice of detergent and concentration dependency for intimin-EE and Fab/EE complexation were worked out by Ivan Morales alongside the scFv/EE variant complexation trials. As in intimin-EE & scFv/EE variant complexation, intimin-EE and Fab/EE complexation was not observed in LDAO detergent on the S300 column, but was observed in DDM detergent on the S12 column. Intimin-EE and Fab/EE complexation showed a much greater concentration dependency than the intimin-EE and scFv/EE complexations. In fact, amount of intimin-EE & Fab/EE complex formed was shown to be linearly dependent upon the concentration of Fab/EE in the mixture (data not shown).

S12 complexations of DDM solubilized WT intimin, intimin-EE7, and intimin-EE8 with Fab/EE are shown in Figure 4.4. Gel filtration and SDS-PAGE analysis revealed intimin-EE7 and intimin-EE8 to form complexes with Fab/EE as compared with the negative control. LDAO solubilized intimin-EE and Fab/EE S12 complexation trials were not performed because observation of complex formation was deemed highly unlikely. Similar to the scFv/EE complexations, a single gel filtration elution peak was not observed for intimin-EE with Fab/EE. A second peak or shoulder peak was observed which was shown to be uncomplexed Fab/EE on the SDS-PAGE gels. Therefore, the

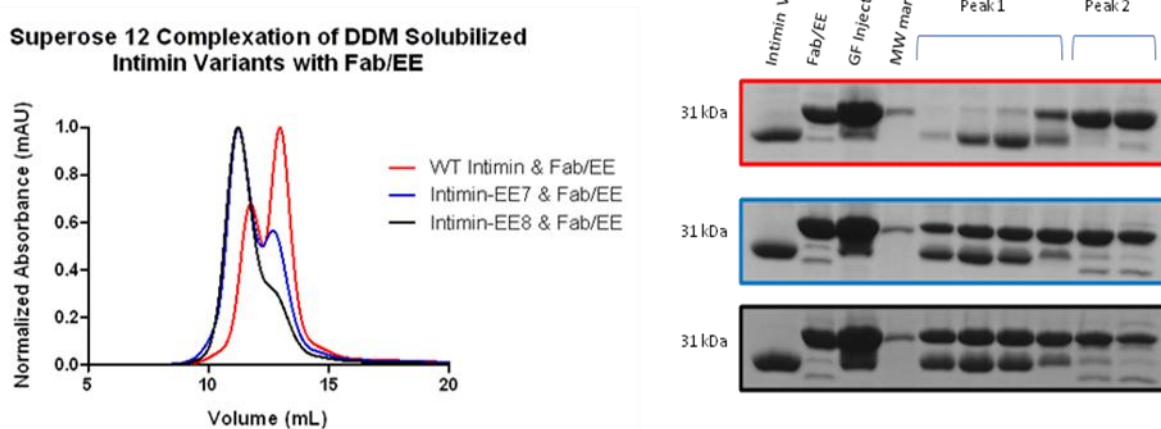


Figure 4.4. Intimin-EE and Fab/EE S12 Complexations

Comparison of S12 gel filtration and SDS-PAGE analysis of DDM solubilized intimin-EE7 and intimin-EE8 with Fab/EE against the negative control. Chromatogram colors are coordinated with their respective gel. Separate elution of WT intimin with Fab/EE was observed as compared to co-elution of intimin-EE variants with Fab/EE. Peak 2 absorbance significantly decreased coupled with a shift in elution volume of peak 1 for both intimin-EE complexations. SDS-PAGE analysis reveals co-elution of proteins in peak 1 with similar band intensity. Therefore complexation occurs when intimin-EE is solubilized in DDM detergent. Peak 1 and Peak 2 corresponds to ~12mL and ~13mL elution volumes respectively.

binding of intimin-EE and Fab/EE may not be 1:1 or the real concentration of intimin-EE was not exactly measured due to possible interference of the detergent micelles.

As a summary, Intimin-EE and scFv/EE variant complexation did not occur when intimin-EE was solubilized in LDAO detergent. This lack of complex formation was found to be independent of scFv/EE identity and type of gel filtration column (S300 or S12). However, the complexation event was observed for both S300 and S12 gel filtrations when intimin-EE was solubilized in DDM detergent. An equilibrium was found to exist between the complex and its individual constituents which could be driven to complex formation by Le Chatelier's Principle. Intimin-EE also forms a complex with Fab/EE when solubilized in DDM detergent. Interestingly, the complexation of both intimin-EE with scFv/EE and Fab/EE was not in a 1:1 ratio due to the observation of uncomplexed scFv/EE and Fab/EE.

CHAPTER 5

CO-CRYSTALLIZATION OF INTIMIN-EE PROTEIN WITH SCFV/EE.K AND FAB/EE ANTIBODY FRAGMENTS

Abstract

Co-crystallization trays of the DDM solubilized intimin-EE protein were prepared for the intimin-EE7 & scFv/EE.k complex, intimin-EE7 & Fab/EE complex, and the intimin-EE8 & Fab/EE complex. DMPC/CHAPSO detergent bicelle trays were prepared for the intimin-EE8 & Fab/EE complex. For the intimin-EE7 & Fab/EE and the intimin-EE8 & Fab/EE complexes, lipid cubic phase (LCP) crystallization trays were prepared in the Center for Structural Biology at The University of Alabama Birmingham. The intimin-EE & antibody fragment complex was either mixed in a 1:1 molar ratio in the crystallization well (1:1 direct mix method), or incubated in a 1:1 molar ratio and isolated via Superose 12 gel filtration (GF method). Crystallization hits were not observed for the intimin-EE7 & 3D5/EE_48 complex produced by either method. A LCP or bicelle crystal hit was not observed for the Fab/EE complexes. For the DDM solubilized intimin-EE8 & Fab/EE complex, crystals were observed in 0.1M NaOAc (pH 4.6), and 20% (v/v) MPD. The tray was prepared in a 1:1 direct mix fashion. Unfortunately, these crystals dissolved back into solution for unknown reasons. Intimin-EE7 & Fab/EE crystals were observed in 0.1M Tris-HCl (pH 8.5), 0.2M TMAO, and 20% (w/v) PEG MME 2000. The intimin-EE7 was solubilized in DDM detergent and the tray was prepared using the 1:1 direct mix method. However, a control crystallization tray in the same condition produced Fab/EE crystals of similar size and shape which strongly suggests the original co-crystals to be just Fab/EE.

Introduction

In order to obtain an atomic model of a protein or protein complex, a common methodology is X-ray crystallography. In such a method, a crystal of the protein of interest is grown, harvested, and shot with X-rays. Data sets of the inflection points (reflections of the X-rays off of the protein electrons) are collected. Depending on the quality of the data, the data set is processed and refined to reveal a protein atomic model. For atomic structural characterization of the intimin-EE & scFv/EE.k and/or the intimin-EE & Fab/EE complex, X-ray crystallography was the method of choice. This chapter details the experimental procedures and results obtained from the co-crystallization trials of the intimin-EE & scFv/EE.k protein complex and the intimin-EE & Fab/EE protein complex

Experimental

Co-crystallization trays were prepared with the intimin-EE7 and intimin-EE8 protein with both scFv/EE.k and Fab/EE proteins. Large scale crystallization trays (sparse matrices) were prepared utilizing the Art Robbins Crystal Gryphon instrument. The sparse matrix trays were the sitting drop vapor diffusion Art Robbins Instruments Intelli-Plate 96. Sparse matrix conditions were commercial screens purchased from Hampton Research, Emerald Biosystems, Rigaku, and Molecular Dimensions (see Appendix D tables for specific screens used). Optimization trays were prepared in Hampton Research cryschem plate (sitting drop). The chemical conditions for each manual optimization tray were prepared from stock solutions. Lipidic Cubic Phase (LCP) sparse matrices were prepared in the Center for Structural Biology at The University of Alabama Birmingham. Hampton Research LCP sandwich plates were used and setup with the Art Robbins

Gryphon LCP instrument. The LCP sparse matrix conditions were LCP commercial screens produced by Molecular Dimensions. All crystal trays were imaged with the Rigaku Minstrel DT Benchtop protein crystal drop imager and recorded in CrystalTrak software. Detailed information concerning each prepared tray can be found in Tables D.1- D.10 in Appendix D.

Results & Discussion

Co-crystallization Trials of Intimin-EE7 & scFv/EE.k

Despite conducting numerous complexation experiments of all the intimin-EE variants with both the scFv/EE and scFv/EE.k variants, only scFv/EE.k entered crystallization trials. This was decided based on its higher protein yield and apparent higher purity upon SDS-PAGE analysis. Only the intimin-EE7 variant underwent co-crystallization trials with scFv/EE.k. This was decided based upon the higher yield obtained with intimin-EE7.

To identify chemical conditions suitable for intimin-EE7 & scFv/EE.k co-crystal growth, sparse matrix trays using commercial crystallization screens were used to screen a large number of chemical conditions. The intimin EE7 and scFv/EE.k complex was prepared in two different ways for the crystallization trials. The complex was isolated by S12 gel filtration, or the intimin EE7 and scFv/EE.k were mixed directly in the crystallization well (1:1 direct mix). A total of 11 sparse matrix trays were prepared along with 3 optimization sitting drop manual trays. The incubation temperature for all crystal trays was room temperature. Four of the sparse matrices were prepared after S12 gel filtration of the intimin-EE7 & scFv/EE.k complex while the other seven were prepared with the 1:1 direct mix method. The optimization trays were prepared with a condition

containing HEPES (pH 7.0), NaCl, and 2-methyl-2, 4-pentenediol (MPD). These trays were prepared for a possible microcrystal hit from a sparse matrix, but co-crystals were not observed. Table D.1 and Table D.2 in Appendix D documents all of the trays prepared for intimin-EE7 & scFv/EE.k

Co-crystallization Trials of Intimin-EE8 & Fab/EE

Crystallization trials for the intimin-EE8 & Fab/EE complex began with a crystallization condition discovered by Ivan Morales for intimin-EE8 & Fab/EE at room temperature. This condition was 0.03M Citrate (pH 4.0), 0.1M KCl, 0.15M MgCl₂, and 43% (v/v) polyethylene glycol 400 (PEG 400) when intimin-EE8 and Fab/EE were mixed in a 1:1 molar ratio in the crystallization well. The intimin-EE8 was solubilized in DDM detergent. The observed crystals were circular in shape, and a low resolution X-ray diffraction pattern was acquired (data not shown). Although circular crystals are not promising candidates for data collection and structure determination, further optimization can be done to obtain possible good-quality crystals. Therefore, the same sitting drop tray was prepared in order to reproduce the intimin-EE8 & Fab/EE crystals, and the same tray was prepared for the Intimin-EE7 & Fab/EE complex. The Intimin-EE8 & Fab/EE crystals could not be reproduced. However, circular crystals were observed for the Intimin-EE7 & Fab/EE complex at room temperature (discussed in next sub-section). A total of four new sparse matrices were prepared for the intimin-EE8 & Fab/EE complex. The intimin-EE8 protein was solubilized in DDM detergent. Three of the sparse matrices were prepared by mixing the protein in a 1:1 molar ratio in the crystallization well, and the other was prepared after S12 GF complex formation. Two sparse matrix hits were

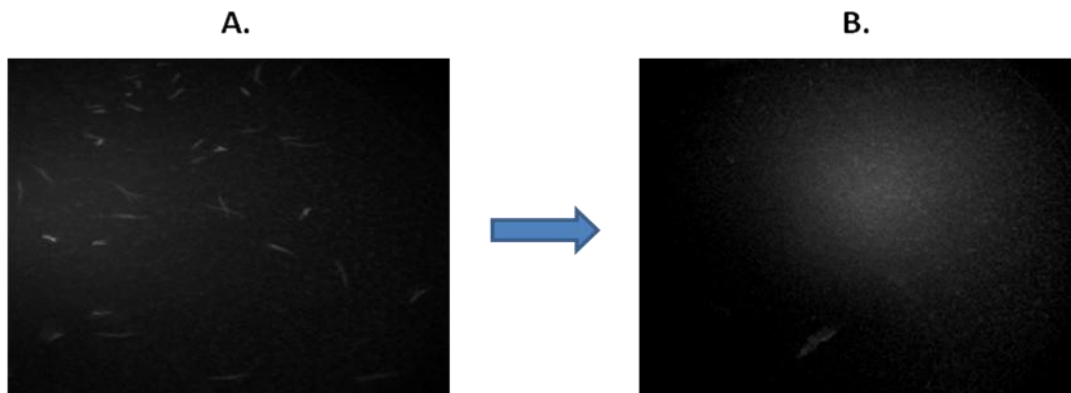


Figure 5.1. Intimin-EE8 and Fab/EE Co-crystal Hit

- A. UV image of the Intimin-EE8 & Fab/EE complex crystals in 0.1M NaOAc (pH 4.6), and 20% (v/v) MPD at room temperature. The crystals were first observed 11 days after tray preparation. The UV image shows rod-like/needle cluster crystals dispersed throughout the crystallization medium.
- B. UV image of the same crystallization well in which the crystals shown in A) were first observed. This image was taken on day 13 after tray preparation. The crystals dissolved in the crystallization medium.

observed for the Intimin-EE8 & Fab/EE complex when the proteins were mixed directly in the crystal well in a 1:1 molar ratio. Both crystal hits were obtained at room temperature. The first crystal condition was 0.1M NaOAc (pH 4.6), 0.02M CaCl₂, and 30% (v/v) MPD, and the second condition was 0.1M HEPES (pH 7.5), 0.2M NaCl, and 35% (v/v) MPD. For both conditions, the crystals appear small in size and circular. From these two new crystal hits, it appeared that the complex favored MPD as a precipitant and a chloride containing salt.

An optimization tray was prepared for each new crystal condition, in which the spindle cluster crystals shown in Figure 5.1 were observed at room temperature in 0.1M NaOAc (pH 4.6) and 20% (v/v) MPD. These crystals appeared in 11 days. Unfortunately, to reasons unknown, the spindle cluster crystals disappeared two days later, and did not re-nucleate. Initially, it was hypothesized that a change in temperature could have caused the crystals to dissolve. In response, the crystal condition was re-made and set at 4°C,

16°C, 20°C, and room temperature. The tray set at room temperature was a control tray in which one row contained only Fab/EE, another only Intimin-EE8, and the last containing Intimin-EE8 and Fab/EE. This control was made in response to the concerns of the crystals actually being the complex, and just not Fab/EE or intimin-EE. An additive screen sparse matrix was also prepared and set at room temperature. An additive screen contains various chemicals which may improve the crystal quality in a known crystallization condition. However, the crystals did not re-appear in any of the temperature screen trays or additive screen, and the Fab/EE and Intimin-EE8 rows in the control tray contained no crystals. These results indicated that the crystals may have been the Intimin-EE8 & Fab/EE complex, but were very sensitive to a variable that changed over the course of two days.

In a second attempt to reproduce the notoriously known “disappearing crystals”, all the temperature screens (RT, 4°C, 16°C, 20°C) along with a second additive screen were prepared for the DDM solubilized intimin-EE8 with Fab/EE in 0.1M NaOAc (pH 4.6), and 20% (v/v) MPD. A buffer/pH screen was prepared in which pH values between 4.0 and 7.5 were tested. A MPD/PEG (low molecular weight) screen was also prepared using MPD, PEG 400, PEG MME 550, and PEG 1000 as precipitating agents. Unfortunately, not a single crystal was observed. All crystal trays prepared for the DDM solubilized intimin-EE8 & Fab/EE complex are recorded in Table D.3 and D.4 in Appendix D.

Due to the fact that excess detergent in the crystallization solution could have been interfering in the crystallization of the complex, alternative crystallization methods were attempted. These alternative methods included DMPC/CHAPSO detergent bicelles,

and lipidic cubic phase (LCP). Both the bicelle and LCP techniques utilize lipids that form bilayers. It was thought that mimicking the natural lipidic environment of the *E. coli* outer membrane with an artificial bilayer would stabilize the intimin-EE protein increasing the possibility of co-nucleation with Fab/EE. A total of five sparse matrices were prepared in which the intimin-EE8 was solubilized in detergent bicelles. The ratio between intimin-EE8 to bicelle was 1:4 in all sparse matrices. The incubation temperature for the trays was room temperature. Four of the sparse matrices contained a final concentration of 8% for the DMPC/CHAPSO bicelles, and one sparse matrix contained a final concentration of 5%. The complex of intimin-EE8 & Fab was prepared in a 1:1 direct mix fashion for all bicelle trays. It should be noted that Ujal et al. reported that final bicelle concentrations between 2-8% could be used, but lower concentration protein samples should use higher final bicelle concentrations.⁽²²⁾ Because of the concentration restraints of the 1:1 direct mix method (Fab/EE concentration cannot exceed 8 mg/mL due to its solubility limit, therefore for a 1:1 molar ratio, the concentration of intimin-EE8 is much lower than 8 mg/mL), the bicelle concentration of 8% was determined to be appropriate. Unfortunately, no bicelle co-crystals were observed. For the LCP method, a total of 4 sparse matrixes were prepared using the 1:1 direct mix method. The monoolein: complex ratio for each tray was 60:40. The incubation temperature for the LCP trays was 20°C. No LCP intimin-EE8 & Fab/EE co-crystals were observed. The bicelle trays prepared are tabulated in Appendix D Table D.5 and the intimin-EE8 & Fab LCP trays in Appendix D Table D.6.

Co-crystallization Trials of Intimin-EE7 & Fab/EE

As discussed in the intimin-EE8 & Fab/EE co-crystallization section, the 0.03M Citrate (pH 4.0), 0.1M KCl, 0.15M MgCl₂, and 43% (v/v) PEG 400 sitting drop vapor diffusion tray was prepared for the intimin-EE7 & Fab/EE complex. Circular crystals were observed for the Intimin-EE7 & Fab/EE complex at room temperature. The crystals appeared in a condition containing 0.03M Citrate (pH 4.0), 0.1M KCl, 0.1M MgCl₂, and 28% (v/v) PEG 400 when Intimin-EE7 and Fab/EE were mixed in a 1:1 molar ratio in the crystallization well. A similar, low resolution X-ray diffraction pattern was obtained for these Intimin-EE7 & Fab/EE crystals. This condition was not optimized further for intimin-EE7 & Fab/EE due to the observed similar diffraction quality as compared to the original intimin-EE8 & Fab/EE crystals (data not shown).

In total, ten sparse matrix trays were prepared for the intimin-EE7 & Fab/EE complex with the intimin-EE7 solubilized in DDM detergent. The incubation temperature for all the sparse matrices was room temperature. Half of the sparse matrix trays were prepared after S12 gel filtration of the intimin-EE7 & Fab/EE complex, and half were prepared by the 1:1 direct mix method. As compared with the intimin-EE8 & Fab/EE 1:1 direct mix crystal trays, the Fab/EE concentration was increased to approximately 8 mg/mL (the highest concentration before Fab/EE would crash out of solution). A crystal hit was observed in a sparse matrix using the Index HT screen produced by Hampton Research. The condition was composed of 0.1M Tris-HCl (pH 8.5), 0.2M trimethylamine N-oxide (TMAO), and 20% (w/v) polyethylene glycol monomethyl ether 2000 (PEG MME 2000). The tray formed the complex in the 1:1 direct mix approach. The incubation temperature was room temperature, and the crystals appeared between 4-15 days and had

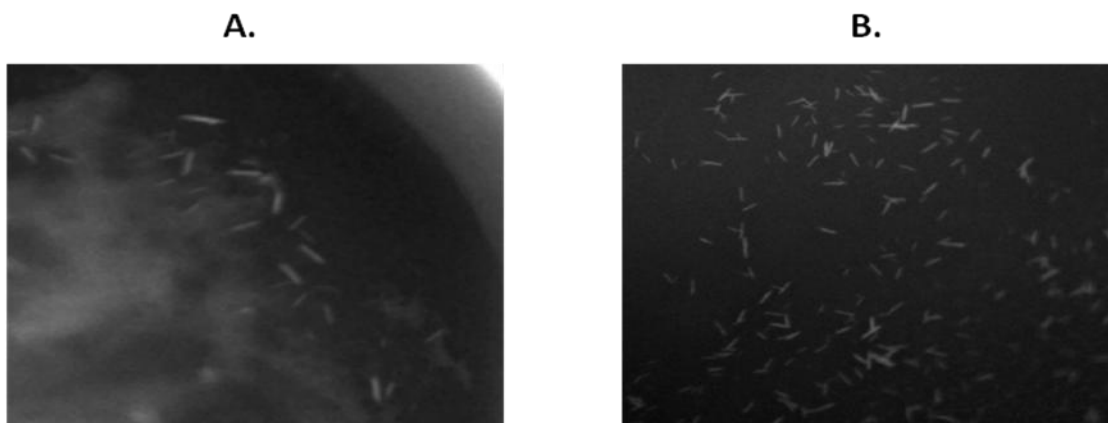


Figure 5.2. Intimin-EE7 and Fab/EE Co-crystal Hit

- A. UV image of the Intimin-EE7 & Fab/EE complex crystals in 0.1M Tris-HCl (8.5), 0.2M TMAO, 20% (w/v) PEG MME 2000 at room temperature. The crystals were observed between 4-15 days after tray preparation. The UV image shows rod-like crystals dispersed in the precipitated crystallization medium.
- B. UV image of Fab/EE crystals in Tris-HCl, TMAO, PEG MME 2000 condition. These Fab/EE crystals have roughly the same size and morphology as the crystals in A. Therefore, it is suggested that the crystals in A. are just Fab/EE.

a maximum length of 60 micrometers (μm). Several sitting drop vapor diffusion optimization trays were prepared for this condition with both the GF complex and 1:1 direct mix approach, yet the crystals could not be reproduced. A control tray in which one row containing Fab/EE, one row containing intimin-EE7, and one row containing intimin-EE7 & Fab/EE was produced. Unfortunately, crystals were observed in the row containing Fab/EE that had approximately the same size and shape of the original sparse matrix crystals. This result implied that the original crystals observed in the sparse matrix were probably Fab/EE. No crystals were observed in the control tray in the intimin-EE7 row or the intimin-EE7 & Fab/EE row. The original sparse matrix hit along with the Fab/EE control crystals are shown in Figure 5.2. Diffraction data from crystals in Figure 5.2 is shown in Appendix D Figure D.1. In all, 19 co-crystallization trays were prepared for the intimin-EE7 & Fab/EE complex with the intimin-EE7 solubilized in DDM detergent. All 19 trays are tabulated in Appendix D Table D.7-D.9.

As with the intimin-EE8 & Fab/EE complex, LCP sparse matrix trays were prepared for the intimin-EE7 & Fab/EE complex. Bicelle crystallization was not attempted for intimin-EE7 & Fab/EE. A total of four LCP trays were prepared, and the incubation temperature was 20°C. The protein: monoolein ratio was 60:40 for all the trays, and the complex formation technique was 1:1 direct mix. No LCP crystals were observed. The LCP trays are recorded in Appendix D Table D.10.

CHAPTER 6

CONCLUSIONS AND FUTURE DIRECTIONS FOR EYMPME PEPTIDE-SPECIFIC CO-CRYSTALLIZATION OF INTIMIN

Despite screening thousands of different crystallization conditions, different incubation temperatures, protein concentrations, and three different crystallization techniques (DDM detergent, DMPC/CHAPSO bicelles, lipidic cubic phases), structure determination quality diffraction data could not be obtained for either the intimin-EE & scFv/EE variant complexes or the intimin-EE & Fab/EE complex. As described by Johnson et al., molecular dynamic (MD) studies were performed for WT intimin, intimin-EE7, and intimin-EE8, and the intimin-EE8 & Fab/EE complex.⁽¹⁸⁾ The purpose of the MD studies was to gain insight into why a co-crystal could be not grown despite strong evidence from gel filtration and SDS-PAGE analysis that the complex was forming in solution.

It was a central point of the proposed EE peptide-specific co-crystallization method that the scFv/EE variants or Fab/EE would strongly bind to the EE containing loop of the membrane protein and form strong crystal contacts. Such a hypothesis would predict a strong EE interaction and formation of a protein complex with limited flexibility. Therefore, the prediction of this conformational rigidity was the purpose of the MD studies. When analyzing the root mean square fluctuation (RMSF) of WT intimin residues 315-320 (L4 loop), the flexibility of these residues were found to increase upon EYMPME mutation. Even though the L4 loop of intimin-EE8 was 4 residues longer (alanine extender sequences) than intimin-EE7, the flexibility of its L4 loop was comparable to that of intimin-EE7. Intermolecular interactions analysis revealed that

within the WT intimin L4 loop, Serine 316 (S316) formed a hydrogen bonding interaction that stabilized the loop. This hydrogen bond was broken when S316 was mutated to tyrosine (Y) in intimin-EE7 and intimin-EE8. MD simulations in which the EE interaction was modeled with Fab/EE showed that the flexibility of the L4 loop moderately increased upon Fab/EE complexation. A portion of the MD data is presented in Figure 6.1 (page 47).

The MD data revealed that insertion of the EE tag removed native interactions of the intimin L4 loop (reference Figure 3.1.A for WT intimin topology diagram), and conformational heterogeneity increased as result. Complexation with Fab/EE did not stabilize the L4 loop, but flexibility slightly increased with formation of the EE complex. Because the scFv/EE variants interact with intimin-EE through the EE interaction, these results are expected to occur with the intimin-EE & scFv/EE variant complexes too. Having a large number of possible conformations for any macromolecular crystallographic study is undesired, and sometimes detrimental as can be seen with intimin-EE.

Despite these unforeseen (and hard to predict) complications with the EE peptide-specific co-crystallization of intimin-EE, this proof-of-concept project may succeed with some future directions. Additional protein engineering of intimin-EE can be performed to reduce the conformational heterogeneity, possibly resulting in the nucleation of a more stable intimin-EE & anti-EE antibody fragment complex. Some possible experiments include truncation of the intimin-EE L4 loop to a minimum number of residues on either side of the EE tag. Several intimin-EE7 or intimin-EE8 variants could be developed each with a different number of L4 residues. Such truncations could “stiffen” the loop

reducing its conformational heterogeneity. On the other side of the EE complex, different antibody fragments could be tested. Additional fragments could include nanobodies (reference Figure 1.1) or darbins. With all of these proposed future experiments, complexation trials for every intimin-EE variant & antibody fragment complex should be performed as discussed in Chapter 3. To further explore the EE interaction, peak 1 fractions can be combined after SDS-PAGE analysis and run over the GF column again. Such experiments will provide additional insight into how tight the intimin-EE & antibody fragment interaction is and enrich the amount of complex in the final solution. At that time, it may be advantageous to perform additional detergent screens. Even though complexations occur with DDM solubilized intimin-EE, DDM may not be the optimal detergent for co-crystallization trials. A detergent screening assay should be performed for each intimin-EE variant developed. Non-detergent crystallization techniques such as LCP can be explored and optimized further. All future detergent and non-detergent (bicelle, LCP, etc) crystallization trials can be performed with the GF protein complex. It can be seen from this work that higher protein concentrations with decreased conformational heterogeneity will be needed for successful co-crystallization.

Our scFv/EE and Fab/EE engineering efforts has led to a high affinity binding site capable of complexation with a purified, detergent-solubilized, EE-tagged membrane protein. As a proof-of-concept for the EE peptide-specific co-crystallization method, the *E. coli* β -barrel membrane protein intimin was chosen as the model membrane protein. Several intimin-EE variants were developed by site directed mutagenesis. intimin-EE7 and intimin-EE8 variants were shown to complex with both scFv/EE.k and Fab/EE when solubilized in DDM detergent. Despite thousands of co-crystallization trials, few

promising results were obtained probably due to the high conformational heterogeneity. Protein engineering efforts for intimin-EE and different antibody fragments may be required for the successful co-crystallization of intimin-EE. Despite the unforeseen complications of this EE co-crystallization method, it is a crystallization method that is attempting to solve one of the most difficult problems in membrane protein structure determination. Even though this method is not ready for high-throughput use today, method optimization can render its use in the future. The purpose of this work was to provide scientific knowledge, a piece of the puzzle, that can be used in the broader goal of EE peptide-specific co-crystallization becoming one of the general membrane protein crystallization methods.

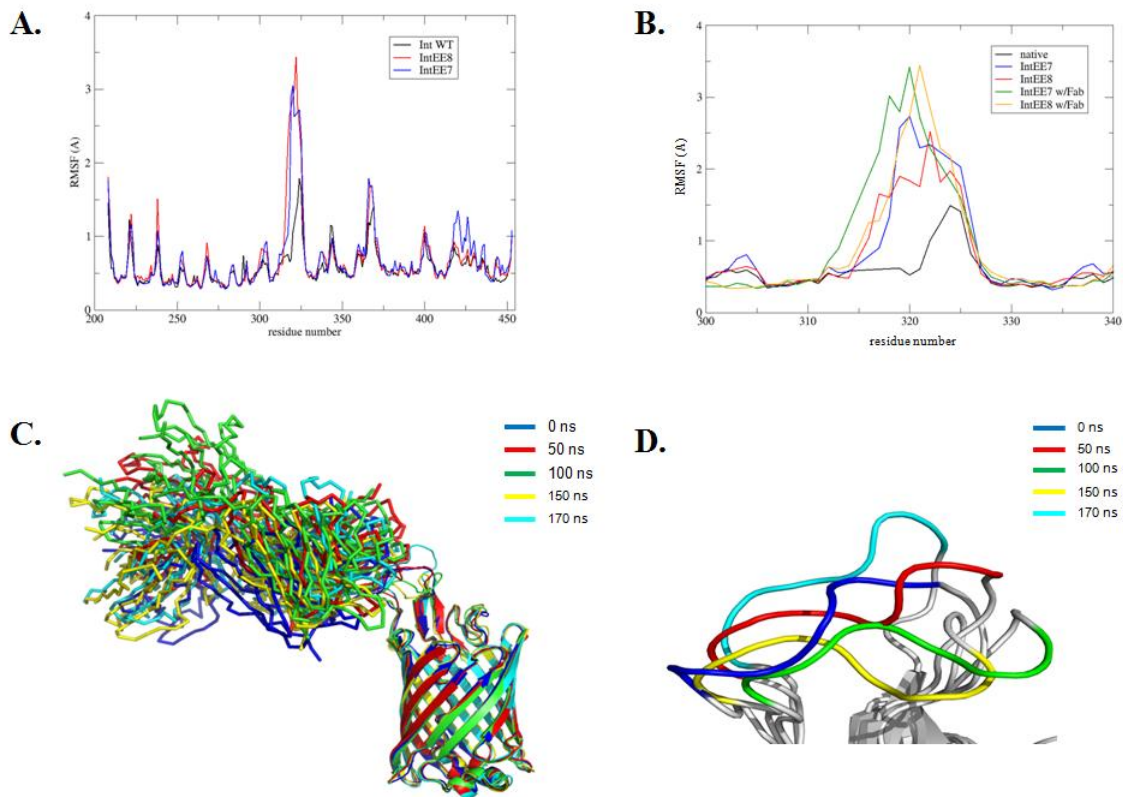


Figure 6.1. Molecular Dynamics of Intimin-EE and Fab/EE

- A. Root mean squared fluctuation (RMSF) of intimin residues 200-450 for WT intimin (black), intimin-EE7 (blue), and intimin-EE8 (red). Flexibility of residues 315-320 (in L4 loop) is seen to increase for intimin-EE7 and intimin-EE8 compared to WT intimin. RMSF for intimin-EE7 and intimin-EE8 are comparable.
- B. RMSF of residues 300-340 for WT intimin (black), intimin-EE7 (blue), intimin-EE8 (red), intimin-EE7 & Fab/EE (green), and intimin-EE8 & Fab/EE (yellow). Flexibility of the L4 loop is seen to moderately increase upon complexation with Fab/EE for both intimin-EE7 and intimin-EE8.
- C. Overlay of intimin-EE8 & Fab/EE MD simulations for 0ns - 170ns. The position of the Fab/EE protein is seen to change which causes conformational heterogeneity in the intimin-EE8 & Fab/EE complex.
- D. Zoom-in of the EE tag in intimin-EE8 & Fab/EE MD simulations for 0ns – 170ns. The two alanine extender sequences flanking both sides of the EE tag are not shown for clarity. Over time, the conformation of the EE tag is changing which can be due to the mutation of S316 to tyrosine eliminating the stabilizing hydrogen bond of the L4 loop.

APPENDIX A

CHAPTER 2 SUPPLEMENTARY

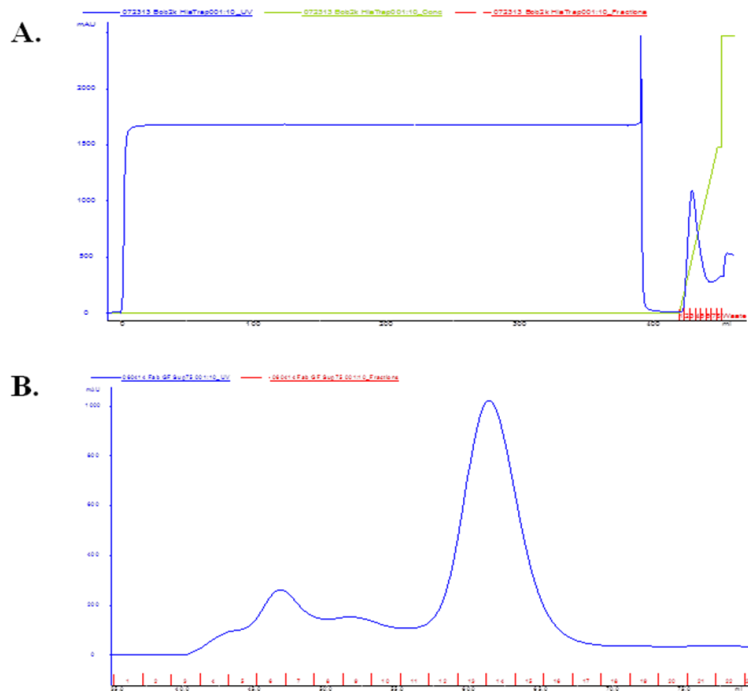


Figure A.1. ScFv/EE.k and Fab/EE Purification Chromatograms

- A. Nickel Affinity Chromatogram for scFv/EE.k. Protein was then buffer exchanged into HBS
- B. Sup75 gel filtration of Fab/EE. Protein was first purified by batch purification (manual nickel affinity)

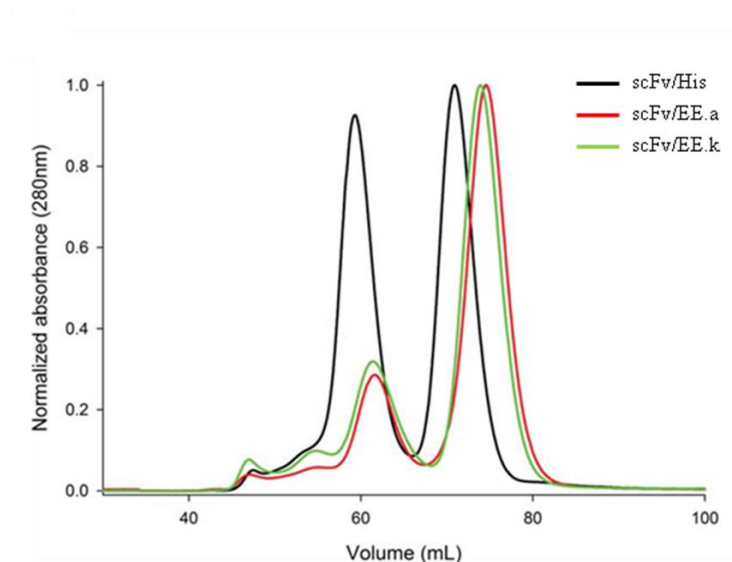


Figure A.2. Oligomeric Analysis of ScFv Variants

Gel filtration of scFv variants on Sup75 column. Peak 1 corresponds to dimeric state of scFv, and Peak 2 corresponds to monomeric state of the scFv. The dimeric state was observed to decrease for the second generation scFv/EE proteins compared with scFv/His. Figure was taken and amended from Kalyoncu et al.⁽¹⁸⁾

Table A.1. ScFv Variant and Fab/EE Protein Yields

	scFv/His ^a	scFv/EE ^a	scFv/EE.k ^b	scFv/EE.a ^b	Fab/EE ^c
Yield (mg protein/ L culture)	8.5	2.1	3.6	0.5	2.4

a. Reference 16 b. Reference 17 c. Reference 18

APPENDIX B

CHAPTER 3 SUPPLEMENTARY

Protein Engineering of Intimin-EE Variants

WT Intimin	HHHHHHHHHENLYFQSMQHYGTAEVNLQSGNNFDGSSLDLFLPFYDSEKMLAFGQVGARYID SRFTANLGAQRFFLPANMLGYNVFDQDFSGDNTRLGIGGEYWRDYFKSSVNGYFRMSGWHE SYNKKDYDERPANGFDIRFNGYLPSPALGAKLIYEQYYGDNVALFNSDKLQSNPGAATVGVNY TPIPLVTMGIDYRHGTGNENDLLYSMQFRYQFDKSWSQIEPQYVNELRTLGSRYDLVQRNNI ILEYK
Intimin-EE1	HHHHHHHHHENLYFQSMQHYGTAEVNLQSGNNFDGSSLDLFLPFYDSEKMLAFGQVGARYID SRFTANLGAQRFFLPANMLGYNVFDQDFSGDNTRLGIGGEYWRDYFKSSVNGYFRMSGWHE SYNKKDYDERPANGFDIRFNGYLPSPALGAKLIYEQYYGDNVALFNSDKLQSNPGAATVGVNY TPIPLVTMGIDYRHGTGNENDLLYSMQFRYQFDKSEYMPMEPQYVNELRTLGSRYDLVQRNN IILEYK
Intimin-EE3	HHHHHHHHHENLYFQSMQHYGTAEVNLQSGNNFDGSSLDLFLPFYDSEKMLAFGQVGARYID SRFTANLGAQRFFLPANMLGYNVFDQDFSGDNTRLGIGGEYWRDYFKSSVNGYFRMSGWHE SYNKKDYDERPANGFDIRFNGYLPSPALGAKLIYEQYYGDNVALFNSDKLQSNPGAATVGVNY TPIPLVTMGIDYRHGTGNENDLLYSMQFRYQFDKSWSQIEPQYVNEYMPMEGSRYDLVQRNN NIILEYK
Intimin-EE4	HHHHHHHHHENLYFQSMQHYGTAEVNLQSGNNFDGSSLDLFLPFYDSEKMLAFGQVGARYID SRFTANLGAQRFFLPANMLGYNVFDQDFSGDNTRLGIGGEYWRDYFKSSVNGYFRMSGWHE SYNKKDYDERPANGFDIRFNGYLPSPALGAKLIYEQYYGDNVALFNSEYMPMEPGAATVGVN YTPIPLVTMGIDYRHGTGNENDLLYSMQFRYQFDKSWSQIEPQYVNELRTLGSRYDLVQRNN NIILEYK
Intimin-EE7	HHHHHHHHHENLYFQSMQHYGTAEVNLQSGNNFDGSSLDLFLPFYDSEKMLAFGQVGARYID SRFTANLGAQRFFLPANMLGYNVFDQDFSGDNTRLGIGGEYWRDYFKSSVNGYFRMSGWHE YMPMEDYDERPANGFDIRFNGYLPSPALGAKLIYEQYYGDNVALFNSDKLQSNPGAATVGVN YTPIPLVTMGIDYRHGTGNENDLLYSMQFRYQFDKSWSQIEPQYVNELRTLGSRYDLVQRNN NIILEYK
Intimin-EE8	HHHHHHHHHENLYFQSMQHYGTAEVNLQSGNNFDGSSLDLFLPFYDSEKMLAFGQVGARYID SRFTANLGAQRFFLPANMLGYNVFDQDFSGDNTRLGIGGEYWRDYFKSSVNGYFRMSGWHA AEMPMEEAADYDERPANGFDIRFNGYLPSPALGAKLIYEQYYGDNVALFNSDKLQSNPGAATV GVNYTPIPLVTMGIDYRHGTGNENDLLYSMQFRYQFDKSWSQIEPQYVNELRTLGSRYDLVQ RNNNIILEYK

Figure B.1. Primary Protein Structure of Intimin Variants

The amino acid sequence (N-terminus → C-terminus) for each intimin variant

Table B.1. Intimin-EE Oligonucleotide Primer Sequences

DNA sequence of the sense and antisense primers for each intimin-EE variant. Nucleotides in yellow encode for the EE tag, and the green sequences for intimin-EE8 encode for the two alanine extenders.

Intimin Variant	Sense and Antisense Primers
EE1	Sense: 5'-AGCATGCAGTTTCGTTACCAGTTCGATAAATCTGAGTATATGCCGATGGAAACCGCAGTATGTGAATGAACTGCGTACC-3'
	Antisense: 5'-GGTACGCAGTTCATTACATACTGCGGTTCATCGGCATATACTCAGATTTATCGAACTGGTAACGAACTGCATGCT-3'
EE3	Sense: 5'-CTTGGAGTCAGCAGATTGAACCGCAGTATGTGAATGAATATATGCCCATGGAGGGTTCTCGCTACGATCTGGTTCAGCGTAACAACA-3'
	Antisense: 5'-TGTTGTTACGCTGAACCGATCGTAGCGAGAACCCTCCATGGGCATATATTCATTACATACTGCGGTTCAATCTGCTGACTCCAAG-
EE4	Sense: 5'-ACAGTATTACGGTGATAATGTGGCCCTGTTAACTCTGAGTATATGCCAATGGAAACCGGGCCGAGCGACGGTGGG-3'
	Antisense: 5'-CCCACGTCGCTGCGCCCGGTTCATTGGGCATATACTCAGAGTTAACAGGGCCACATTATCACCGTAATACTGT-3'
EE7	Sense: 5'-CGGCTACTTCCGTATGAGTGGTTGGCATGAATACATGCCCATGGAAAGATTACGATGAACGCCCGGCAAATGGCTTTGATATTCG-3'
	Antisense: 5'-CGAATATCAAAGCCATTTGCCGGGCGTTCATCGTAATCTTCCATGGGCATGTATTCATGCCAACCACTCATACGGAAGTAGCCG-3'
EE8	Sense: 5'-CGGCTACTTCCGTATGAGTGGTTGGCATGCGGCGGAATACATGCCCATGGAAAGCGGCGGATTACGATGAACGCCCGGCAAATGGC-3'
	Antisense: 5'-GCCATTTGCCGGGCGTTCATCGTAATCGCGCGCTTCCATGGGCATGTATTCGCGCGCATGCCAACCACTCATACGGAAGTAGCCG-

Expression and Purification of Intimin-EE Variants

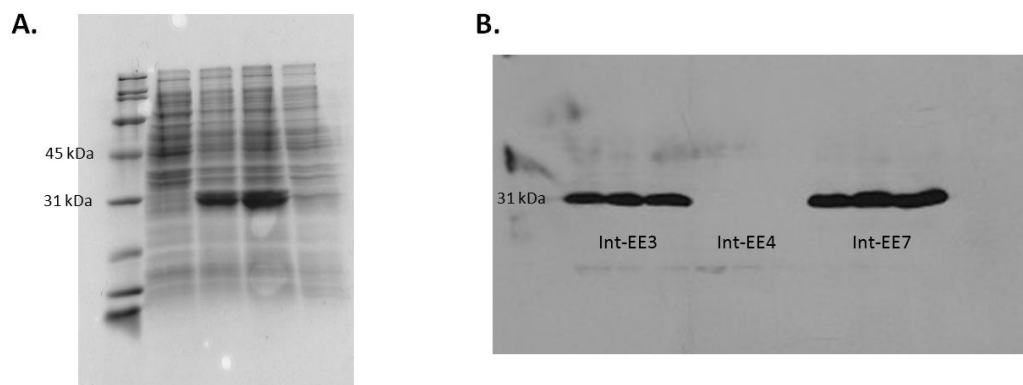


Figure B.2. Intimin-EE Variant Expression

- SDS-PAGE for the expression of intimin-EE1 within 4 different *E. coli* colonies after thermal treatment. The large bands for the two colonies in the middle of the gel (31 kDa) correspond to intimin-EE1.
- Western blot analysis for the expression of intimin-EE3, intimin-EE4, and intimin-EE7 colonies. For each variant, 3 *E. coli* colonies were tested. All three colonies for intimin-EE3 and intimin-EE7 express the protein; however, intimin-EE4 was not expressed.

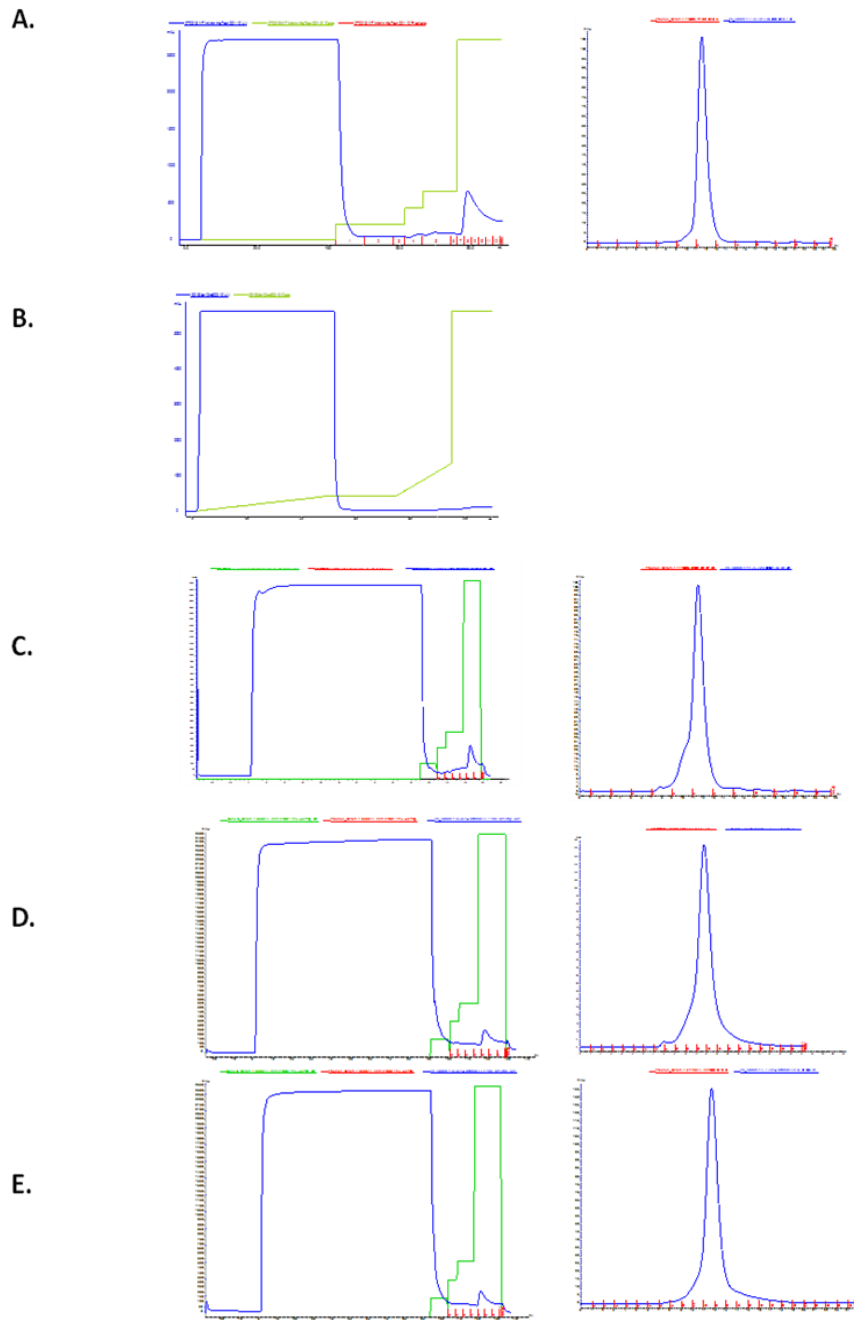


Figure B.3. Intimin Variant Purification Chromatograms

- A. Ni-NTA and S12 chromatograms for WT intimin. (07/02/13 purification)
- B. Ni-NTA of intimin-EE3 (03/12/13 purification)
- C. Ni-NTA and S12 chromatograms for intimin-EE1 (11/26/13 purification)
- D. Ni-NTA and S12 chromatograms for intimin-EE7 (05/06/14 purification)
- E. Ni-NTA and S12 chromatograms for intimin-EE8 (05/06/14 purification)

Table B.2. LDAO Solubilized Intimin Variant Protein Yields

Intimin variant yields when solubilized in LDAO detergent. Some purifications performed by Ivan Morales.

Purification Date	Variant	Membrane: (g)	Yield: (mg)	$\frac{\text{protein (mg)}}{\text{membrane (g)}}$
1/24/13	WT	3.20	1.200	0.375
3/12/13	EE3	3.56	0	0
3/12/13	EE7	3.75	2.266	0.604
5/29/13	EE8	4.30	2.78	0.647
6/6/13	EE1	4.13	0.590	0.143

Table B.3. DDM Solubilized Intimin Variant Protein Yields

Intimin variant yields when solubilized in DDM detergent.

Purification Date	Variant	Membrane (g)	Yield (mg)	$\frac{\text{protein (mg)}}{\text{membrane (g)}}$
7/02/13	WT	3.10	~1.00	0.323
6/18/14	EE7	3.89	2.02	0.519
5/09/14	EE8	4.55	0.969	0.213
11/22/13	EE1	3.97	0.800	0.202

APPENDIX C

CHAPTER 4 SUPPLEMENTARY

Table C.1. All Intimin-EE and ScFv/EE Variant S300 Complexations
S300 complexations of intimin-EE variants with scFv/EE variants.

Intimin Variant	Detergent	scFv/EE Variant
WT Intimin	LDAO	scFv/EE and scFv/EE.k
	DDM	scFv/EE.k
Intimin-EE1	LDAO	scFv/EE.k
Intimin-EE7	LDAO	scFv/EE and scFv/EE.k
	DDM	scFv/EE.k
Intimin-EE8	LDAO	scFv/EE.k
	DDM	scFv/EE.k

Table C.2. All Intimin-EE and ScFv/EE.k S12 Complexations
S12 complexations of intimin-EE variants with scFv/EE variants.

Intimin Variant	Detergent	scFv/EE Variant
WT Intimin	LDAO	scFv/EE.k
	DDM	scFv/EE.k
Intimin-EE1	DDM	scFv/EE.k
Intimin-EE7	LDAO	scFv/EE.k
	DDM	scFv/EE.k
Intimin-EE8	DDM	scFv/EE.k

APPENDIX D

CHAPTER 5 SUPPLEMENTARY

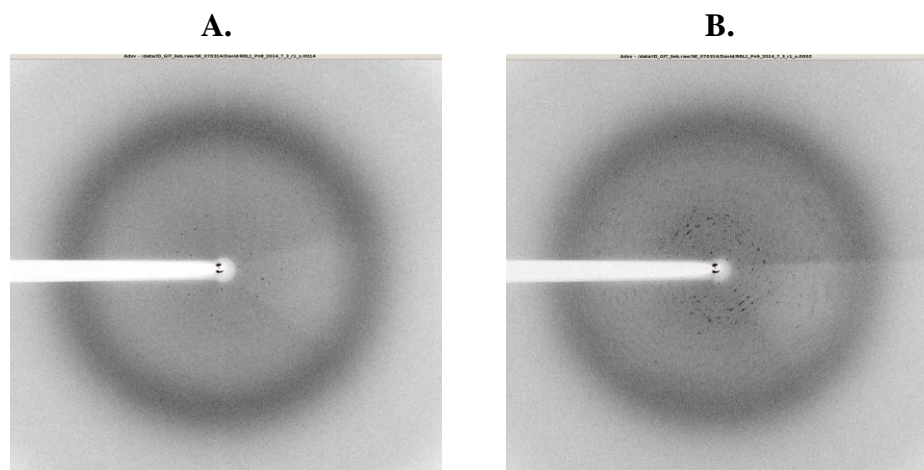


Figure D.1. Diffraction of Intimin-EE7 and Fab/EE Co-crystal Hit

(A) Diffraction obtained for Intimin-EE7 & Fab/EE co-crystal hit

(B) Diffractions obtained from Fab/EE Control. Dot smearing may be due to DDM detergent in solution

Table D.1. Co-Crystallization Trays Prepared for DDM Solubilized intimin-EE7 & scFv/EE.k

Preparation date (Tray #)	Manual Optimization/ Sparse matrix screen	Crystallization condition	Complex formation	Concentration Intimin-EE7 stock (mg/mL)	Concentration scFv/EE.k stock (mg/mL)	Temperature (°C)
07-26-2013	MembFac	N/A	Gel filtration	Complex: 6.89		RT
08-30-2013	MembFac	N/A	Gel filtration	Complex: 10.37		RT
09-13-2013	MemPlus	N/A	Gel filtration	Complex: 10.70		RT
09-13-2013	Index HT	N/A	Gel filtration	Complex: 6.26		RT
09-25-2013 (5)	MemPlus	N/A	1:1 direct mix	5.68	5.43	RT
09-25-2013 (6)	MembFac	N/A	1:1 direct mix	5.68	5.43	RT
10-02-2013 (7)	MemPlus	N/A	2:1 direct mix	2.84	5.43	RT

**Table D.2. Co-Crystallization Trays Prepared For DDM Solubilized Intimin-EE7 & scFv/EE.k
Continued**

Preparation date (Tray #)	Manual Optimization/ Sparse matrix screen	Crystallization condition	Complex formation	Concentration Intimin-EE7 stock (mg/mL)	Concentration scFv/EE.k stock (mg/mL)	Temperature (°C)
10-18-2013 (M.T. 1)	Manual Optimization	0.1M HEPES (7.0) 0.1-0.4 M NaCl 29-39% MPD	Gel filtration	Complex: 10.73		RT
10-23-2013 (M.T. 2)	Manual Optimization	0.1M HEPES (7.0) 0.1-0.4M NaCl 29-39% MPD	1:1 direct mix	5.68	5.43	RT
11-06-2013 (8)	MemGold	N/A	1:1 direct mix	5.68	5.43	RT
11-06-2013 (9)	HR2-130	N/A	1:1 direct mix	5.68	5.43	RT
11-06-2013 (10)	MemPlus	N/A	1:1 direct mix	5.68	5.43	RT
11-13-2013 (M.T. 3)	Manual Optimization	0.1M HEPES (7.0) 0.34-0.40M NaCl 31-36% MPD	1:1 direct mix	5.68	5.43	RT
11-13-2013 (11)	PEG/Ion	N/A	1:1 direct mix	5.68	5.43	RT

Table D.3. Co-crystallization trays prepared for DDM solubilized intimin-EE8 & Fab/EE

Preparation date (Tray #)	Manual Optimization/ Sparse matrix screen	Crystallization condition	Complex formation	Concentration Intimin-EE8 stock (mg/mL)	Concentration Fab/EE stock (mg/mL)	Temperature (°C)
02-07-2014 (1)	Manual Optimization	0.03M Citrate pH 4.0, 0.1M KCl, 0.10M-0.25M MgCl ₂ , 23%-48% (v/v) PEG 400	1:1 direct mix	4.22	7.60	RT
02-14-14 (2)	HR2-130	N/A	1:1 direct mix	3.97	7.16	RT
02-14-2014 (3)	PEG Rx HT	N/A	1:1 direct mix	3.97	7.16	RT
02-14-2014 (4)	Wizard I & II	N/A	1:1 direct mix	3.97	7.16	RT
03-07-2014	MembFab	N/A	Gel filtration	Complex: 7.60		RT
03-14-2014 (5)	Manual Optimization	0, 0.1M NaOAc (4.6) 0,0.02,0.05,0.1M CaCl ₂ 15-40% MPD	1:1 direct mix	3.97	7.16	RT
03-14-2014 (6)	Manual Optimization	0.1M HEPES (7.5) 0.1-0.4M NaCl 20-45% MPD	1:1 direct mix	3.97	7.16	RT
04-04-2014 (7)	Manual Optimization	0.1M NaOAc (4.6) 16-26% MPD	1:1 direct mix	3.85	6.94	4
04-04-2014 (8)	Manual Optimization	0.1M NaOAc (4.6) 16-26% MPD	1:1 direct mix	3.85	6.94	20
04-04-2014 (9)	Manual Optimization	0.1M NaOAc (4.6) 16-26% MPD	1:1 direct mix	3.85	6.94	16
04-04-2014 (10)	Manual Optimization	0.1M NaOAc (4.6) 16-26% MPD	1:1 direct mix Control tray→ A) Fab B) EE8 C) EE8+Fab	3.85	6.94	RT

**Table D.4. Co-crystallization Trays Prepared for DDM Solubilized Intimin-EE8 & Fab/EE
Continued**

Preparation date (Tray #)	Manual Optimization/ Sparse matrix screen	Crystallization condition	Complex formation	Concentration Intimin-EE8 stock (mg/mL)	Concentration Fab/EE stock (mg/mL)	Temperature (°C)
04-04-2014 (11)	Additive Screen	0.1M NaOAc (4.6) 16-26% MPD	1:1 direct mix	3.85	6.94	RT
05-14-2014 (13)	Manual Optimization	0.1M NaOAc (4.6) 16-26% MPD	1:1 direct mix Control tray #2→ A) Fab B) EE8 C) EE8+Fab	3.97	7.16	RT
05-15-2014 (14)	Manual Optimization	0.1M NaOAc (4.6) 16-26% MPD	1:1 direct mix	A) 7.16 B) 8.07	A) 3.97 B) 4.48	RT
05-15-2014 (15)	Manual Optimization	0.1M NaOAc (4.6) 16-26% MPD	1:1 direct mix	3.97	7.16	4
05-15-2014 (16)	Manual Optimization	0.1M NaOAc (4.6) 16-26% MPD	1:1 direct mix	3.97	7.16	20
05-15-2014 (17)	Manual Optimization	0.1M NaOAc (4.6) 16-26% MPD	1:1 direct mix	3.97	7.16	16
05-16-2014 (18)	Manual Optimization	A: 0.1M NaOAc (4.0) B: 0.1M NaOAc (4.6) C: 0.1M BisTris (6.5) D: 0.1M HEPES (7.5) 17-32% MPD	1:1 direct mix pH Screen	3.97	7.16	RT
05-16-2014 (19)	Manual Optimization	0.1M NaOAc (4.6) A: 15- 40% MPD B: 15-40% PEG 400 C: 15-40% PEG MME 550 D: 15-40% PEG 1000	1:1 direct mix MPD/PEG Screen	3.97	7.16	RT
05-19-2014 (20)	Additive Screen	0.1M NaOAc (4.6) 16-26% MPD	1:1 direct mix	3.97	7.16	RT

Table D.5. Co-crystallization Trays of the DMPC/CHAPSO Bicelle Solubilized Intimin-EE8 & Fab/EE

Preparation date (Tray #)	Sparse matrix screen	Complex formation	Bicelle concentration (%)	Concentration Intimin-EE8 stock (mg/mL)	Concentration Fab/EE stock (mg/mL)	Temperature (°C)
04-18-2014 (12)	MemPlus	1:1 direct mix	8	5.1	6.94	RT
05-19-2014 (21)	MembFac	1:1 direct mix	5	8.07	8.07	RT
05-19-2014 (22)	MemGold	1:1 direct mix	8	8.07	8.07	RT
05-19-2014 (23)	Wizard I & II	1:1 direct mix	8	8.07	8.07	RT
05-19-2014 (24)	MembFac	1:1 direct mix	8	8.07	8.07	RT

Table D.6. LCP Trays Prepared for Intimin-EE8 & Fab/EE

Preparation date	LCP sparse matrix screen	Complex formation	Concentration Intimin-EE8 stock (mg/mL)	Concentration Fab/EE stock (mg/mL)	Monoolein: Complex ratio	Temperature (°C)
05-12-2014	Cubic phase I	1:1 direct mix	8.07	8.07	60:40	20
05-12-2014	Cubic phase II	1:1 direct mix	8.07	8.07	60:40	20
05-12-2014	MB class I	1:1 direct mix	8.07	8.07	60:40	20
05-12-2014	MB class II	1:1 direct mix	8.07	8.07	60:40	20

Table D.7. Co-crystallization Trays Prepared for DDM Solubilized Intimin-EE7 & Fab/EE

Preparation date (Tray #)	Manual Optimization/ Sparse matrix screen	Crystallization condition	Complex formation	Concentration Intimin-EE7 stock (mg/mL)	Concentration Fab/EE stock (mg/mL)	Temperature (°C)
02-07-2014 (1)	Manual Optimization	0.03M Citrate pH 4.0, 0.1M KCl, 0.10M-0.25M MgCl ₂ , 23%-48% (v/v) PEG 400	1:1 direct mix	4.22	7.60	RT
02-18-2014 (2)	MemPlus	N/A	1:1 direct mix	3.97	7.16	RT
03-07-2014 (3)	MembFac	N/A	Gel filtration	Complex: 10.76		RT
03-07-2014 (4)	Manual Optimization	0.1M NaOAc (4.6) 16-26% MPD	1:1 direct mix	3.97	7.16	RT
05-20-2014 (5)	MemGold	N/A	1:1 direct mix	4.48	8.07	RT
05-20-2014 (6)	MembFac	N/A	1:1 direct mix	4.48	8.07	RT
05-20-2014 (7)	Wizard I & II	N/A	1:1 direct mix	4.48	8.07	RT
05-20-2014 (8)	Index HT	N/A	1:1 direct mix	4.48	8.07	RT
06-06-2014 (9)	Manual Optimization	0.1M Tris-HCl (8.5) 12-28%, 30% PEG 2000 MME A: 0.1M TMAO B: 0.2M TMAO C:0.25M TMAO D: 0.3M TMAO	1:1 direct mix	4.30	7.74	RT

**Table D.8. Co-crystallization Trays Prepared for DDM Solubilized Intimin-EE7 & Fab/EE
Continued**

Preparation date (Tray #)	Manual Optimization/ Sparse matrix screen	Crystallization condition	Complex formation	Concentration Intimin-EE7 stock (mg/mL)	Concentration Fab/EE stock (mg/mL)	Temperature (°C)
06-09-2014 (10)	Manual Optimization	0.1M Tris-HCl (8.5) 12-28%,30% PEG 2000 MME 0.2M TMAO	1:1 direct mix Control tray → A: Fab B: EE7 C: EE7 & Fab	4.30	7.74	RT
06-11-2014 (11)	Manual Optimization	0.1M Tris-HCl (8.5) 0.2M TMAO A) 12-28%, 30% PEG 550 MME B) 12-28%, 30% PEG 1000 C) 12-28%, 30% PEG 2000 MME D) 12-28%, 30% PEG 4000	1:1 direct mix PEG screen	4.30	7.74	RT
06-11-2014 (12)	Manual Optimization	0.2M TMAO 12-28%, 30% PEG 2000 MME A: 0.1M citric acid (5.5) B: 0.1M MOPS (7.0) C: 0.1M Tris-HCl (8.5) D: 0.1M Glycine (9.5)	1:1 direct mix Buffer screen	4.30	7.74	RT
06-16-2014 (13)	Manual Optimization	0.1M Tris-HCl (8.5) 12-28%, 30% PEG 2000 MME A: 0.1M TMAO B: 0.2M TMAO C: 0.25M TMAO D: 0.3M TMAO	1:1 direct mix	4.40	7.90	RT

Table D.9. Co-crystallization Trays Prepared for DDM Solubilized Intimin-EE7 & Fab/EE Continued

Preparation date (Tray #)	Manual Optimization/Sparse matrix screen	Crystallization condition	Complex formation	Concentration Intimin-EE7 stock (mg/mL)	Concentration Fab/EE stock (mg/mL)	Temperature (°C)
06-16-2014 (14)	Sparse matrix	A1) Well F2 mother liquor A2) My own optimization mother liquor	1:1 direct mix	4.40	7.90	RT
06-19-2014 (15)	MemPlus	N/A	Gel filtration	Complex: 12.65		RT
06-25-2014 (16)	Cryo I & II	N/A	Gel filtration	Complex: 11.37		RT
06-27-2014 (17)	Wizard III & IV	N/A	Gel filtration	Complex: 12.10		RT
06-27-2014 (18)	PEG/Ion	N/A	Gel filtration	Complex: 10.74		RT
07-01-2014 (19)	Manual Optimization	A: 0.2M MgCl ₂ , 10-35% PEG 3350 B: 0.2M NaH ₂ PO ₄ , 10-35% PEG 3350 C: 0.1M Tris-HCl (8.5); 0.2M TMAO; 12-28%, 30% PEG 2000 MME	Gel filtration	Complex: 11.31		RT

Table D.10. LCP Trays Prepared for Intimin-EE7 & Fab/EE

Preparation date	LCP sparse matrix screen	Complex formation	Concentration Intimin-EE7 stock (mg/mL)	Concentration Fab/EE stock (mg/mL)	Monoolein: Complex ratio	Temperature (°C)
05-12-2014	Cubic phase I	1:1 direct mix	7.05	8.07	60:40	20
05-12-2014	Cubic phase II	1:1 direct mix	7.05	8.07	60:40	20
05-12-2014	MB class I	1:1 direct mix	7.05	8.07	60:40	20
05-12-2014	MB class II	1:1 direct mix	7.05	8.07	60:40	20

REFERENCES

- [1] Kendrew, J. C., Bodo, G., Dintzis, H. M., Parrish, R. G., and Wyckoff. (1958) A Three Dimensional Model of the Myoglobin Molecule obtained by X-ray Analysis, *Nature* 181, 662-666.
- [2] Koszelak-Rosenblum, M., Krol, A., Mozumdar, N., Wunsch, K., Ferin, A., Cook, E., Veatch, C. K., Nagel, R., Luft, J. R., De Titta, G. T., and Malkowski, M. G. (2009) Determination and application of empirically derived detergent phase boundaries to effectively crystallize membrane proteins, *Protein Sci.* 18, 1828-1839.
- [3] Lieberman, R. L., Culver, J. A., Entzminger, K. C., Pai, J. C., and Maynard, J. A. (2011) Crystallization chaperone strategies for membrane proteins, *Methods* 55, 293-302.
- [4] Mancina, F., and Love, J. (2010) High-throughput expression and purification of membrane proteins, *J. Struct. Biol.* 172, 85-93.
- [5] Newby, Z. E. R., O'Connell, J. D., III, Gruswitz, F., Hays, F. A., Harries, W. E. C., Harwood, I. M., Ho, J. D., Lee, J. K., Savage, D. F., Miercke, L. J. W., and Stroud, R. M. (2009) A general protocol for the crystallization of membrane proteins for X-ray structural investigation, *Nat. Protoc.* 4, 619-637.
- [6] Love, J., Mancina, F., Shapiro, L., Punta, M., Rost, B., Girvin, M., Wang, D.-N., Zhou, M., Hunt, J. F., Szyperski, T., Gouaux, E., MacKinnon, R., McDermott, A., Honig, B., Inouye, M., Montelione, G., and Hendrickson, W. A. (2010) The New York Consortium on Membrane Protein Structure (NYCOMPS): a high-throughput platform for structural genomics of integral membrane proteins, *J. Struct. Funct. Genomics* 11, 191-199.
- [7] Caffrey, M., and Cherezov, V. (2009) Crystallizing membrane proteins using lipidic mesophases, *Nat. Protoc.* 4, 706-731.
- [8] Faham, S., and Bowie, J. U. (2002) Bicelle crystallization: a new method for crystallizing membrane proteins yields a monomeric bacteriorhodopsin structure, *J. Mol. Biol.* 316, 1-6.
- [9] Cherezov, V., Rosenbaum, D. M., Hanson, M. A., Rasmussen, S. G. F., Thian, F. S., Kobilka, T. S., Choi, H.-J., Kuhn, P., Weis, W. I., Kobilka, B. K., Stevens, R. C., Takeda, S., Kadowaki, S., Haga, T., Takaesu, H., Mitaku, S., Fredriksson, R., Lagerstrom, M. C., Lundin, L. G., Schioth, H. B., Pierce, K. L., Premont, R. T., Lefkowitz, R. J., Lefkowitz, R. J., Shenoy, S. K., and Rosenbaum, D. M. (2007)

High-Resolution Crystal Structure of an Engineered Human β 2-Adrenergic G Protein-Coupled Receptor, *Science* 318, 1258-1265.

- [10] Ujwal, R., Cascio, D., Colletier, J.-P., Faham, S., Zhang, J., Toro, L., Ping, P., and Abramson, J. (2008) The crystal structure of mouse VDAC1 at 2.3 Å resolution reveals mechanistic insights into metabolite gating, *Proc. Natl. Acad. Sci. U. S. A.* 105, 17742-17747.
- [11] Li, X., Dang, S., Chuangye, Y., Gong, X., Wang, J., and Shi, Y. (2013) Structure of a presenilin family intramembrane aspartate protease, *Nature* 493, 56-61
- [12] Derewenda, Z. S. (2004) Rational Protein Crystallization Ways & Means by Mutational Surface Engineering, *Structure* 12, 529-535
- [13] Rasmussen, S. G. F., DeVree, B. T., Zou, Y., Kruse, A. C., Chung, K. Y., Kobilka, T. S., Thian, F. S., Chae, P. S., Pardon, E., Calinski, D., Mathiesen, J. M., Shah, S. T. A., Lyons, J. A., Caffrey, M., Gellman, S. H., Steyaert, J., Skiniotis, G., Weis, W. I., Sunahara, R. K., and Kobilka, B. K. (2011) Crystal Structure of the Beta2 Adrenergic Receptor-Gs Protein Complex, *Nature* 477, 549-555.
- [14] Zhou, Y., Morais-Cabral, J. H., Kaufman, A., and MacKinnon, R. (2001) Chemistry of ion coordination and hydration revealed by a K⁺ channel-Fab complex at 2.0Å resolution, *Nature* 414, 43-48.
- [15] Day, P. W., Rasmussen, S. G. F., Parnot, C., Fung, J. J., Masood, A., Kobilka, T. S., Yao, X.-J., Choi, H.-J., Weis, W. I., Rohrer, D. K., and Kobilka, B. K. (2007) A monoclonal antibody for G protein-coupled receptor crystallography, *Nat Methods* 4, 927-929.
- [16] Pai, J. C., Culver, J. A., Drury, J. E., Motani, R. S., Lieberman, R. L., and Maynard, J. A. (2011) Conversion of scFv peptide-binding specificity for crystal chaperone development, *Protein Eng. Des. Sel.* 24, 419-428.
- [17] Kalyoncu, S., Hyun, J., Pai, J. C., Johnson, J. L., Entzminger, K., Jain, A., Heaner, D. P., Jr., Morales, I. A., Truskett, T. M., Maynard, J. A., and Lieberman, R. L. (2014) Effects of protein engineering and rational mutagenesis on crystal lattice of single chain antibody fragments, *Proteins: Struct. Funct. Bioinf.* 82, 1884-1895.
- [18] Johnson, J.L., Entzminger, K., Hyun, J., Kalyoncu, S., Heaner, D.P.Jr., Morales, I.A., Sheppard, A., Gumbart, J.C., Maynard, J.A., & Lieberman, R.L. (2015) Structural and biophysical characterization of epitope-specific engineered Fab fragment and complexation with membrane proteins: implications for co-crystallization. *Acta Crystallogr. Sect. D: Biol. Crystallogr.* D71, 896-906

- [19] Fairman, J. W., Dautin, N., Wojtowicz, D., Liu, W., Noinaj, N., Barnard, T. J., Udho, E., Przytycka, T. M., Cherezov, V., and Buchanan, S. K. (2012) Crystal Structures of the Outer Membrane Domain of Intimin and Invasin from Enterohemorrhagic *E. coli* and Enteropathogenic *Y. pseudotuberculosis*, *Structure* 20, 1233-1243.
- [20] Roosild, T. P., Castronovo, S., and Choe, S. (2006) Structure of anti-FLAG M2 Fab domain and its use in the stabilization of engineered membrane proteins, *Acta Crystallogr. F-Struct. Biol. Cryst. Commun.* 62, 835-839.
- [21] Kaufmann, M., Lindner, P., Honegger, A., Blank, K., Tschopp, M., Capitani, G., Pluckthun, A., and Grutter, M. G. (2002) Crystal structure of the anti-His tag antibody 3D5 single-chain fragment complexed to its antigen, *J. Mol. Biol.* 318, 135-147.
- [22] Ujwal, R., and Bowie, J. U. (2011) Crystallizing membrane proteins using lipidic bicelles, *Methods* 55, 337-341.

VITA

DAVID P. HEANER JR.

HEANER was born in Atlanta, Georgia. He attended private school in Atlanta, Georgia, and received his B.S. in Chemistry from Georgia Institute of Technology, Georgia in 2015. When he is not working on research, Mr. Heaner enjoys kayaking and hiking with friends and family.